

Accounts

A New Strategy for Construction of Covalently Linked Giant Porphyrin Arrays with One, Two, and Three Dimensionally Arranged Architectures

Naoki Aratani and Atsuhiro Osuka*

Department of Chemistry, Graduate School of Science, Kyoto University, Sakyo-ku, Kyoto 606-8502

(Received February 22, 2001)

Synthesis, structural characteristics, and optical and electrochemical properties of various *meso–meso*-linked porphyrin arrays were described. The Ag^{I}-salt-promoted *meso–meso* coupling reaction of 5,15-diaryl and 5,10,15-triaryl Zn^{II}-porphyrins is advantageous in light of its high regioselectivity as well as its easy extension to large porphyrin arrays. A similar coupling reaction is also possible by electrochemical oxidations for Zn^{II}- and Mg^{II}-porphyrins, while the electrochemical oxidation of Ni^{II}-, Pd^{II}, and Cu^{II}-porphyrins led to formation of *meso*-β linked biporphyrins with high regioselectivity. As an extension of the above Ag^{I}-promoted coupling reaction, 1,4-phenylene-bridged linear porphyrin arrays were coupled to give orthogonally arranged windmill-like porphyrin arrays, which in turn were further coupled to afford grid-like porphyrin arrays of giant size. In all the Zn^{II}-metallated windmill arrays, the intramolecular singlet–singlet excitation energy transfer proceeds efficiently from the peripheral porphyrins to the central biporphyrin core. The doubling reaction was repeated up to the synthesis of 128-mer. During these attempts, many *meso–meso*-linked porphyrin arrays were isolated in a discrete form by repetitive gel-permeation chromatography (GPC)–HPLC, all exhibiting high solubility in common organic solvents in spite of their giant molecular sizes. Finally, the oxidation with strong oxidant tris(4-bromophenyl)aminium hexachloroantimonate allowed the coupling of 5,10,15-triaryl Ni^{II}- and Pd^{II}-porphyrins to *meso*-β doubly-linked fused biporphyrins and the smooth conversion of *meso–meso*-linked Cu^{II}-biporphyrin to *meso–meso* β–β β–β triply-linked biporphyrin. These fused biporphyrins exhibit full π-conjugation over the arrays.

Light-harvesting complexes (LHC) and reaction centers (RC), which are the key players in the primary processes of photosynthesis, constitute well-organized systems in which the chromophores are held at fixed distances and orientations relative to one another.[1–6] It is clear that the well-defined geometry is one of the important factors requisite for efficient and ultrafast energy and/or electron transfer in the natural systems. In order to understand the mechanisms operating in the photosynthetic systems as well as to duplicate the light harvesting and charge separating functions, a variety of artificial models consisting of multi-porphyrins have been explored so far.[7–11] Conformationally restricted face-to-face diporphyrins have also been studied in order to explore efficient four-electron oxygen reduction catalysts.[12]

In recent years, on the other hand, a considerable attention has been focused on the synthesis of monodisperse macromolecular rods of precise length and constitution in light of their potential applications as molecular-scale electronics.[13–17] A goal of modern electronics research is to make working electronic devices as small as possible. Small devices and short connections between them make microelectronic circuits faster and more compact. The smallest possible unit of a material may be a discrete single molecule.[18–27] Many researchers today are exploring the intriguing possibility of making electronic circuit components from single molecules. This kind of engineering on a molecular scale may eventually yield not only tiny versions of conventional devices but also new ones that exploit quantum effects. Another very active area of research is device structures that use *light*, rather than *electrons*, as the medium for carrying information.[28]

Among many molecular modules used as construction elements of supramolecular rods, porphyrins are one of the most attractive building blocks, since they offer a variety of desirable features, such as rigid planar geometry, high stability, intense electronic absorption and emission, small HOMO–LUMO energy gap, and flexible tunability of their optical and redox properties by appropriate metallation.[29–59] As a matter of fact, the preparations of supramolecular porphyrin arrays have increassed recently for the realization of various molecular devices.[7–11] However, these studies are often hampered by poor solubility, difficult separations, and demanding characterizations. Therefore, high solubilities, easy separations, and reliable characterizations of the arrays are of prime importance to explore larger molecular systems.

From 1984, we have continued the synthetic approaches toward photosynthetic reaction centers by synthesizing a variety of electron acceptor–porphyrin compounds and multi-porphyrin arrays to realize the coupled light-harvesting energy trans-

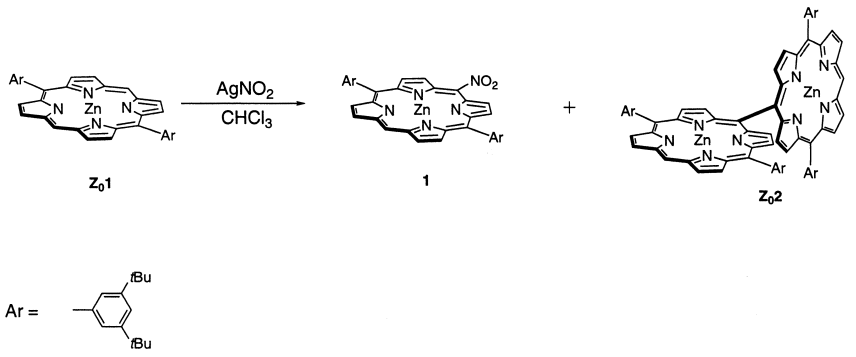

Scheme 1. Reaction of Zn^{II} 5,15-diarylporphyrin with $AgNO_2$.

fer and charge-separating multi-step electron transfer reactions in a single molecule, preferably by way of a reaction sequence that is similar to that in the natural RC's.[60–68] We have developed several model compounds which indeed realized a long-lived charge-separated state in a similar manner to that in RC.[64,66] In the course of these studies, we needed a strongly electron-accepting porphyrin for a study on the energy gap dependence of porphyrin–porphyrin intramolecular electron transfer reaction.[65] We employed Baldwin's conditions[69] ($AgNO_2$ and I_2) for preparation of *meso*-nitrated 5,15-diaryl Zn^{II} porphyrin **1** from $\mathbf{Z_0 1}$. The nitration proceeded nicely to give **1** in 90% yield, but we found the formation of an interesting side product, whose structure turned out to be *meso–meso*-linked biporphyrin $\mathbf{Z_0 2}$ on the grounds of its spectroscopic data (Scheme 1).[38] This reaction was the starting point of our studies on a wide range of *meso–meso*-linked multi-porphyrin arrays.

In this account, the synthesis, the structural characteristics, and the optical and electrochemical properties of *meso–meso*-linked porphyrin arrays and multiply-linked fused porphyrin arrays will be described. As to *meso–meso*-linked porphyrin arrays, we have succeeded in the synthesis of porphyrin 128-mer, which is, to the best of our knowledge, the longest (ca. 100 nm = 0.1 μm) monodisperse rod-like man-made molecule.[45,46] It is interesting to note that even the 128-mer is sufficiently soluble in $CHCl_3$ for many manipulations. This nice solubility must be one key for the successful preparation of the extremely long molecules. With stronger oxidants such as hexachloroantimonate (p-$BrC_6H_4)_3NSbCl_6$ (BAHA), 5,15-diaryl-substituted and 5,10,15-triaryl-substituted metalloporphyrins were coupled to give doubly *meso–β*-linked fused biporphyrins[70,71] and *meso–meso*-linked Cu^{II}-biporphyrin was converted to triply-linked biporphyrin.[72] These oxidative transformations constitute novel routes to fully conjugated electronic systems made of porphyrin π-systems, which are of particular interest for applications in material chemistry as well as molecular electronic devices.

1. Synthesis and Optical Properties of Directly *meso–meso*-Linked Porphyrin Arrays

1-1. Discovery. The formation of **1** in the reaction of $\mathbf{Z_0 1}$ with $AgNO_2$ and I_2 (Scheme 1) can be accounted for in terms of initial one-electron oxidation of $\mathbf{Z_0 1}$ followed by nucleophilic attack by NO_2^-. The observed concurrent formation of $\mathbf{Z_0 2}$ may be explained by a similar mechanism involving the generation of a cation radical of $\mathbf{Z_0 1}$ followed by nucleophilic attack of another neutral molecule of $\mathbf{Z_0 1}$. Based on this consideration, we examined the reaction of $\mathbf{Z_0 1}$ with Ag^I-salts bearing non-nucleophilic anions, such as $AgBF_4$, $AgClO_4$, and $AgPF_6$, which all afforded only *meso–meso*-linked biporphyrin $\mathbf{Z_0 2}$, terporphyrin $\mathbf{Z_0 3}$, and quaterporphyrin $\mathbf{Z_0 4}$.[38] These products were hard to separate on silica gel but could be nicely separated on the size-exclusion chromatography (SEC). Nearly at the same time, Segawa et al. reported the synthesis of *meso–meso*-linked biporphyrin and terporphyrin in low yields by the reaction of *meso*-formylated Cu^{II}-porphyrin with dipyrromethane,[54] and Smith et al. reported the synthesis of analogous *meso–meso*-linked biporphyrin with 1,1,2,2,-tetra(5-formyl-2-pyrrolyl)ethene as a key intermediate.[55]

Initially we employed relatively soluble Zn^{II} 5,15-bis(3,5-di-*t*-butylphenyl)-porphyrin $\mathbf{Z_0 1}$ as the starting substrate. The monomer $\mathbf{Z_0 1}$ was readily prepared from 3,5-di-*t*-butylbenzaldehyde and dipyrromethane in 36% yield under the standard conditions.[73,74] The reaction of $\mathbf{Z_0 1}$ with 0.5 mol amt. of $AgPF_6$ in $CHCl_3$ for 5 h, followed by preparative SEC, gave $\mathbf{Z_0 2}$ in 25% yield, $\mathbf{Z_0 3}$ in 4% yield, and high oligomers along with recovery of $\mathbf{Z_0 1}$ (47%) (Scheme 2). The coupling reaction of $\mathbf{Z_0 2}$ under analogous conditions afforded $\mathbf{Z_0 4}$ in 23% yield. In the ^{1}H NMR spectrum of $\mathbf{Z_0 1}$, a singlet for the *meso*-protons appears at 10.34 ppm and two doublets for the *β*-protons appear at 9.45 and 9.20 ppm. The spectrum of $\mathbf{Z_0 2}$ exhibits a singlet for the *meso*-protons (10.39 ppm) and two doublets for the outer *β*-protons at 9.49 and 9.18 ppm and two doublets for inner *β*-protons at 8.74 and 8.12 ppm, being characteristic of the *meso–meso*-linked biporphyrin. The inner *β*-protons are lying in the shielding region of the neighboring porphyrin. Similarly, a singlet for the *meso*-protons, two doublets for the outer *β*-protons, and 4 kinds of peaks for the inner *β*-protons are observed for $\mathbf{Z_0 3}$. These spectral data are fully consistent with the *meso–meso*-coupled porphyrin arrays.

Here it is worthy of note that *meso*-positions of porphyrins have been known to be the most reactive centers towards both electrophilic and nucleophilic reagents. These reactivities are usually masked in tetraphenylporphyrin (TPP) and octaethylporphyrin (OEP) derivatives because of *ipso*-phenyl groups in the former and the severe steric congestion due to the neighboring *β*-alkyl subsutituents in the latter. In this respect, 5,15-diarylporphyrins, which lack *β*-pyrrolic substituents, are a nice substrate for exploring the intrinsic high reactivity of the *meso*-positions, particularly towards sterically demanding reagents.

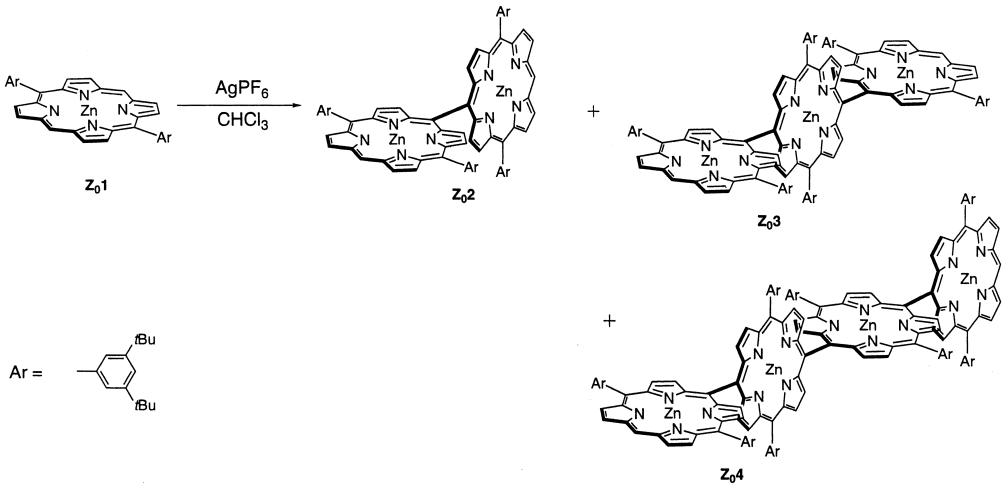

Scheme 2. Ag^{I}-promoted *meso–meso* coupling reaction of Zn^{II} 5,15-diarylporphyrin.

It seems probable that steric congestion around the *meso–meso* linkage in the previously studied bis(tetrapyrroles)[75,76] suppresses the formation of *meso–meso*-linked porphyrins, in which the planarity of porphyrin would increase the steric hindrance.

1-2. Mechanistic Studies on *meso–meso*-Linked Coupling Reactions. The electron transfer-initiated coupling mechanism has also been supported by the following facts. Firstly, the coupling reaction was accelerated and was complete within 5–10 min by addition of I_2. Probably, the reaction of Ag^{I}-ion with I_2 may produce more powerful oxidizing species. Secondly, the same *meso–meso* coupling was also effective by anodic electrochemical oxidation[51,52] (Scheme 3) and by other oxidants.[56–58] An anodic electrochemical oxidation method is useful since the usage of expensive silver salts is not required, and the oxidation potentials can be best tuned to the porphyrin (**2**, **3**, and **4**) which are hardly coupled at all or only slowly coupled in the reaction with $AgPF_6$. In addition, prolonged electrolysis resulted in formation of longer porphyrin arrays (up to octamer $\mathbf{Z_08}$), albeit in quite a low yield.[52]

From a mechanistic point of view, the anodic electrochemical oxidation is of particular interest, since the coupling regioselectivity was found to vary depending upon the central metal ion. The high *meso–meso*-coupling regio-selectivity observed for $\mathbf{Z_01}$ may be explained in term of favorable A_{2u} HOMO orbital. Thus, when Zn^{II}-TPP is oxidized to its radical cation, the corresponding A_{2u} orbital becomes the magnetic orbital.[77,78] Such a cation radical will be attacked by a neutral Zn^{II}-porphyrin at its *meso*-position, which is in this case the most nucleophilic site. Mg^{II}-porphyrin **9** also gave *meso–meso*-linked biporphyrin **14** upon the electrochemical oxidation, but the demetallation by the liberated acid concurrently suppressed the product yield. In sharp contrast, Cu^{II}, Pd^{II}, and Ni^{II} porphyrins (**10**, **11**, and **12**) afforded the corresponding *meso–β* directly linked biporphyrins (**15**, **16**, and **17**) exclusively (Scheme 4).[51] Interestingly, these porphyrins have been shown to favor the A_{1u} HOMO orbitals.[78] Chart 1 shows the A_{2u} and A_{1u} HOMO orbital characteristics. Electron density at the *meso* carbons in A_{2u} is much larger than that at the *β*-pyrrole carbons, whereas in A_{1u} the *meso* carbons become four nodes, resulting in larger electron density at the *β*-pyrrole carbons relative to *meso* carbons. Therefore, the results from the electrochemical oxidation reactions are in line with the proposed mechanism, involving the initial one-electron oxidation of metalloporphyrin followed by nucleophilic attack of a neutral metalloporphyrin at *meso* carbon.

In accord with this mechanistic line, several groups have reported the oxidative synthesis of *meso–meso*-linked biporphyrins. Grazynski et al.[56] used toxic thallium(III) trifluoroacetate oxidant, Liebeskind et al.[57] used 2,3-dichloro-5,6-dicyano-1,4-benzoquinone (DDQ) oxidant, and Senge et al.[58] used DDQ for the oxidation of the corresponding anions.

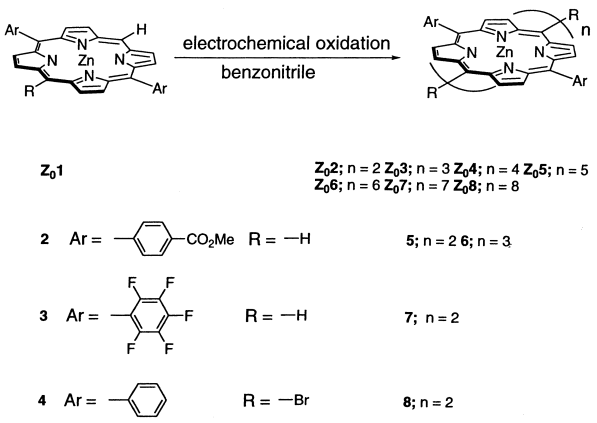

Scheme 3. Electrochemical oxidation of Zn^{II} 5,15-diarylporphyrin.

Chart 1. Schematic presentation of the two HOMO orbitals, A_{1u} and A_{2u} of the D_{4h} porphyrin ring.

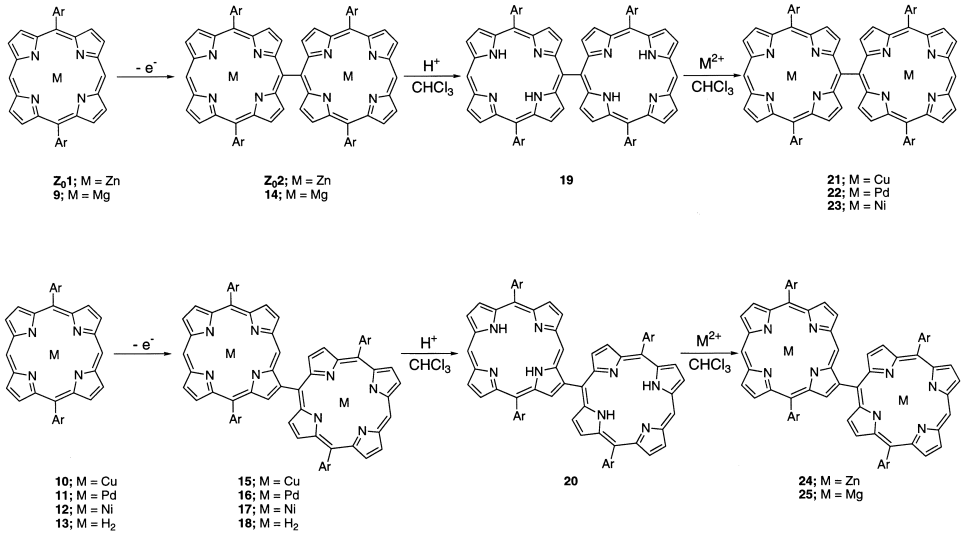

Scheme 4. Regioselective coupling reaction of metallated 5,15-diarylporphyrins, upon electrochemical oxidation.

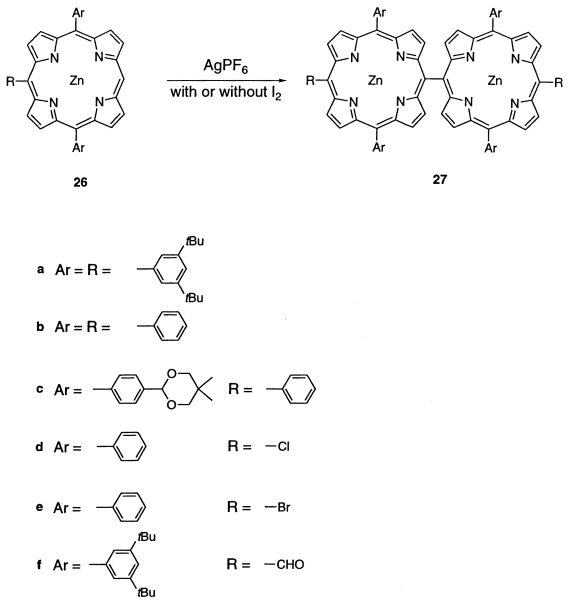

Scheme 5. *meso–meso* Coupling reaction of Zn^{II} 5,10,15-trisubstituted-porphyrins.

In the reaction with $AgPF_6$, 5,15-diarylporphyrinatozincs with two free *meso*-positions tend to react in an extensive manner to give higher oligomers even in the early stage, giving rise to a moderate yield of biporphyrin (ca. 20–30%). On the contrary, 5,10,15-trisubstituted-porphyrins **26** with a single free *meso*-position gave the corresponding biporphyrin **27** in higher yields (65–95%) under the stronger conditions with $AgPF_6$ and I_2 (Scheme 5).[40]

The Ag^I-promoted *meso–meso*-coupling reactions of Zn^{II}-porphyrins normally took 5–10 h with Ag^I salt only and were markedly accelerated (completed within several minutes) by the combined use of Ag^I-salt and iodine as described. These reactions, however, tend to be interrupted due to concomitant liberation of acid that demetallates the reactant Zn^{II}-porphyrin. In order to avoid this demetallation, we attempted to add pyridine to the reaction mixture, which led to complete suppression of the *meso–meso* coupling reaction but resulted in clean *meso*-iodation[79] as a rare example (Scheme 6). At first we thought it may involve in situ formed *N*-iodopyridinium salt as a possible iodinating species. On the basis of this reaction, either the oligoporphyrins or iodoporphyrins could be selectively prepared simply by selecting pure $CHCl_3$ or a mixture of $CHCl_3$ and pyridine as the solvent, respectively. In recent paper, Liebeskind et al. reported the solvent effect on product distribution of this reaction.[57] In non-coordinating solvents such as CH_2Cl_2 and toluene, the reaction of 5,10,15-trisubstituted-porphyrin with I_2/AgO_2CCF_3 gave the porphyrin dimer as the major product. In contrast, in either THF or 1,4-dioxane the iodoporphyrin was the major or the exclusive product. On the basis of these results, Liebeskind et al. suggested pyridine coordination on the zinc ion to be responsible for altering the course of the reaction.

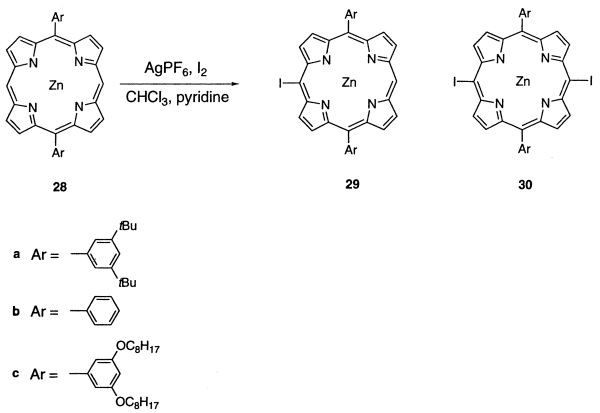

Scheme 6. *meso*-Iodination of Zn^{II} 5,15-diarylporphyrin.

Another interesting aspect of the Ag^I-promoted *meso–meso* coupling reactions is their extension to the preparation of long poly(porphyrinylene)s upon addition of *N*,*N*-dimethylacetamide (DMA) or slight heating. Formally, the formation of one *meso–meso* bond is accompanied by the loss of two hydrogens and thus needs two molar amounts of oxidants. This is nicely illustrated by the reaction of **Z₀1** with 1.5 mol amt. of $AgPF_6$ in

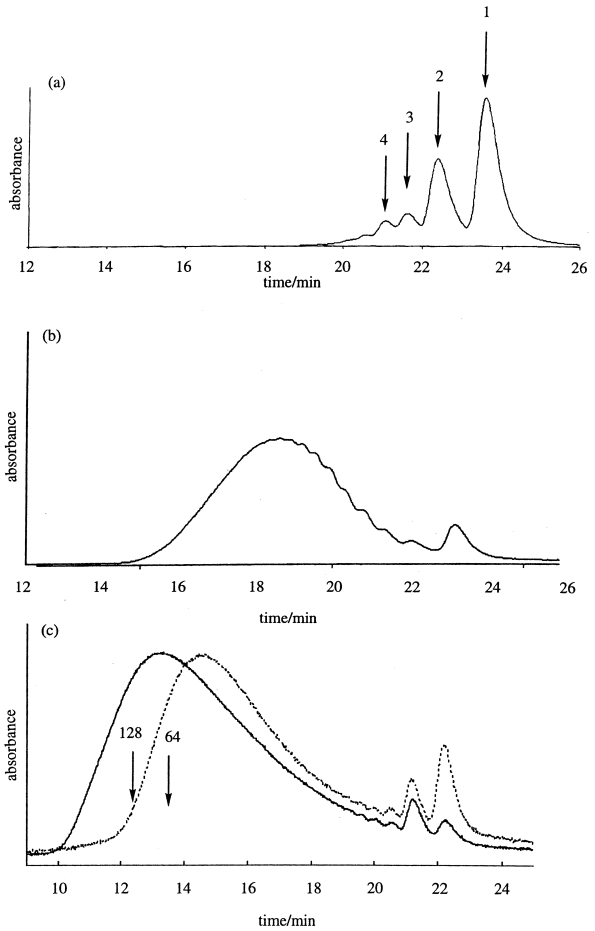

Fig. 1. GPC–HPLC charts of the reaction of **$Z_0$1** and **Z1** with 1.5 eq $AgPF_6$ in $CHCl_3$ detected at 413 nm; (a) **$Z_0$1**, room temperature, 4 h, no DMA, arrows 1-4 indicate the elution bands corresponding to **$Z_0$1**, **$Z_0$2**, **$Z_0$3**, and **$Z_0$4**, respectively. (b) **$Z_0$1**, room temperature, 4 h, 0.5% DMA; (c) **Z1**, 45 °C, 0.5% DMA, 11 h (dotted line); **Z1**, 45 °C, 0.5% DMA, 82 h (solid line), the retention times of discrete 64-mer and 128-mer were indicated by arrows.

$CHCl_3$ at 20 °C for 4 h, which gave **$Z_0$2** (25–30%), **$Z_0$3** (5–7%), and **$Z_0$4** (1–2%) (Fig. 1a). In marked contrast, reaction under the similar conditions but with the presence of a small amount of DMA (0.5% to $CHCl_3$) gave rise to enhanced oligomerization in only 0.5 h, as shown in Fig. 1b and Scheme 7.[44] On the basis of the relationship of the molecular weights of discrete oligo(porphyrinylene)s vs the retention time of GPC/HPLC, M_w = 12000 Da with a polydispersity of 1.46 were estimated. In the polymerization of **$Z_0$1**, the detectable largest oligomers corresponded to about 50-mers. The mechanism of this polymerization has not been clarified yet, but may be accounted for by considering initial one-electron oxidation of Zn^{II}-porphyrin with $AgPF_6$ and subsequent chain elongation processes similar to that proposed for the oxidative formation poly-*para*-phenylenes (PPP).[80] It should be emphasized here that 5,15-diaryl-substituted Zn^{II}-porphyrins like **$Z_0$1** can be polymerized under quite mild conditions in comparison to those used for PPP. With more soluble substrate **Z1**, higher polymer with M_w = 250000 Da and a polydispersity of 2.78 was

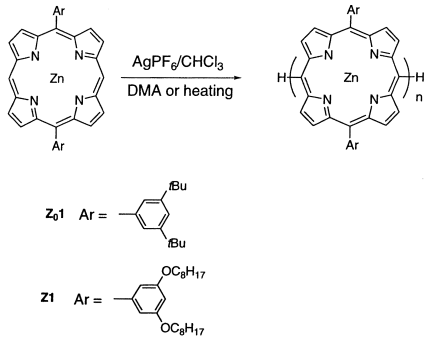

Scheme 7. Ag^{I}-promoted polymerization of Zn^{II} 5,15-diarylporphyrin.

formed under the similar conditions at 45 °C after 82 h (Fig. 1c), where the band top corresponded to about 90-mer.

1-3. Optical Properties of *meso–meso*-Linked Porphyrin Arrays. The *meso–meso*-coupled porphyrin arrays exhibit large splitting of Soret bands due to strong exciton coupling.[81–83] With an increase in the number of porphyrins, the low-energy Soret band is shifted to longer wavelength, while the high-energy Soret band remains at nearly the same wavelength (413–414 nm), resulting in a progressive increase in the splitting energy. The systematic spectral changes can be explained by the simple point-dipole exciton coupling theory developed by Kasha[81] (see section 5-2). Unperturbed Soret transitions at 413–414 nm for all the arrays suggest the averaged perpendicular conformation vice versa. The X-ray crystallography[55,84] and calculation by AM1 method[41] also suggests the orthogonal geometry. When the observed splitting energies were plotted against $\cos[(\pi/(N+1)]$, a nicely straight line with a slope of ΔE_0 = 4250 cm^{-1} was obtained (section 5-2. Fig. 6). The observed linear relationship indicates that the absorption spectral shapes are actually influenced by the number of porphyrins and the constituent porphyrins are regularly aligned in the same linear arrangement in the solution. On this basis, these arrays in the ground state are considered to consist of repeating individual chromophores with substantial electronic interactions.

1-4. Properties of *meso–β*-Linked Biporphyrins. As described above, simple electrochemical oxidation of metalloporphyrin bearing A_{1u}-HOMO orbital (Cu^{II}, Ni^{II}, and Pd^{II}) allows the regioselective synthesis of *meso–β*-linked biporphyrins.[51] Among these, *meso–β*-linked Cu^{II}-biporphyrin was synthetically useful, since it was effectively demetallated to the corresponding free-base porphyrin array **20** from which various metallated *meso–β*-linked biporphyrins including *meso–β*-linked Zn^{II}-biporphyrin **24** and Mg^{II}-biporphyrin **25** can be prepared (Scheme 4).

The *meso–β*-linked Zn^{II}-biporphyrin **24** also displays split Soret bands due to the exciton coupling, but its exciton coupling energy (2530 cm^{-1}) is smaller than that of **$Z_0$2** presumably due to the orientation deviation of transition dipole moments of two porphyrin rings and the slightly longer distance between the two porphyrins that has been estimated to be 8.74 Å from its preliminary X-ray crystallography.

2. Supramolecular Assemblies Based on *meso–meso*-Linked Porphyrins

Molecular assembly using intermolecular interactions has

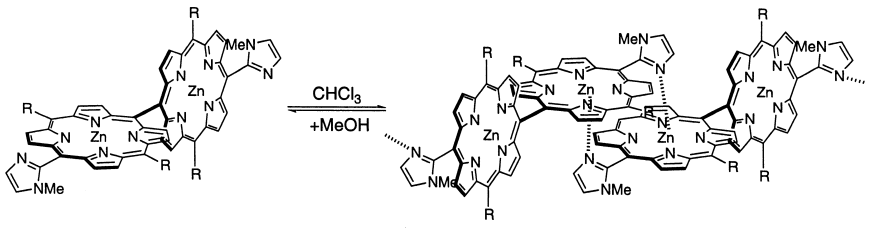

32

Scheme 8. Molecular assembly of *meso–meso*-linked biporphyrin using Zn^{II}-imidazole coordination.

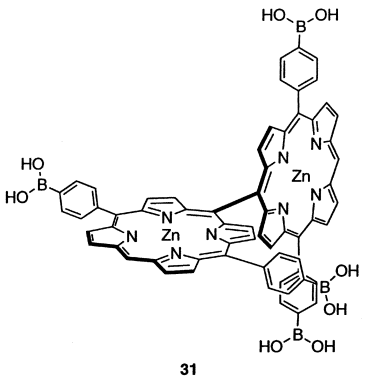

31

Chart 2. Disaccharide host based on *meso–meso*-linked biporphyrin.

been of recent interest as a means of constructing large molecular architectures quickly and efficiently.[85–87] Porphyrins are attractive molecules due to their fascinating photophysical, catalytic, and geometrical properties. For instance, Shinkai et al. reported the usage of *meso–meso*-linked biporphyrin as a "long" and "rigid" scaffold for saccharide recognition (Chart 2).[50] Interestingly, compound **31** shows a high affinity with maltotetraose among the maltooligosaccharides, with appearance of exciton-coupling type circular dichroism (CD) bands in the Soret band region, it is the first artificial saccharide receptor which shows selectivity for oligosaccharides.

Polymer formation in alcohol-free $CHCl_3$ from bis(imidazolylporphyrin) **32** was recently reported; here imidazolyl-Zn coordination bonds were used to connect each part (Scheme 8).[59] Molecular weights of the resulting supramolecular porphyrin complexes analyzed by using GPC were determined as 1×10^5 daltons for the most abundant species, corresponded to the link of about 80 bis(imidazolylporphyrin) units, the molecular length of the porphyrin array has been estimated as 110 nm. On the basis of concentration effect experiments, the complementary coordination is concluded to be complete at concentrations as low as 5.0×10^{-9} M. It is noteworthy that MeOH competes with the imidazolyl group for coordination to the Zn center and can control the degree of organization.

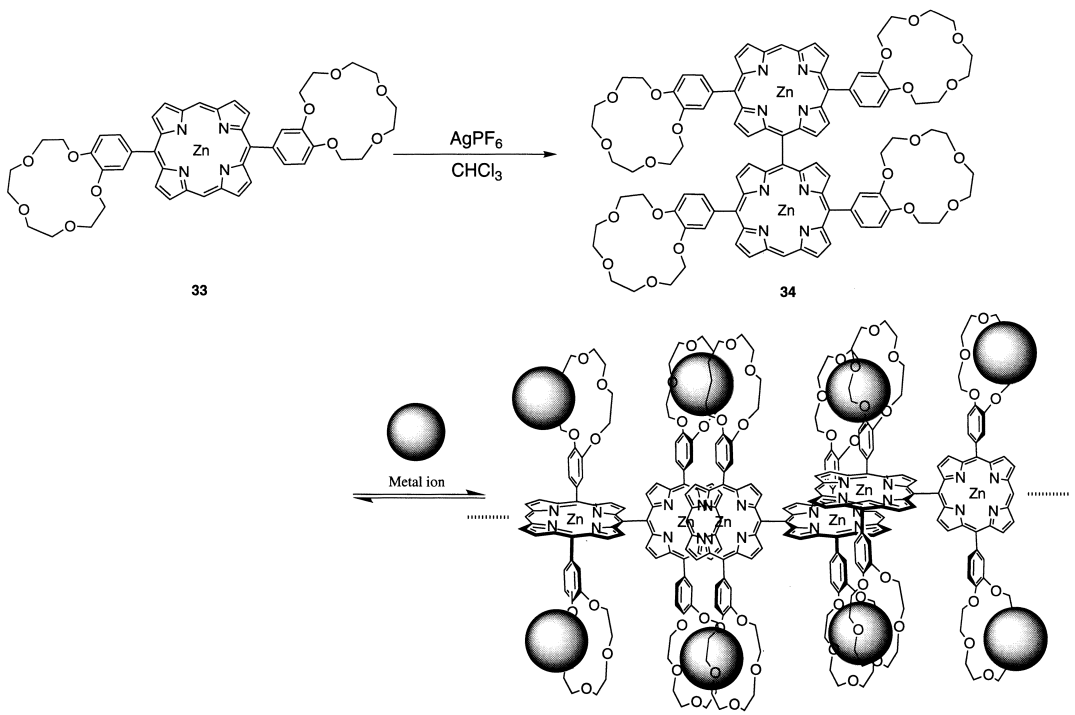

33 **34**

Scheme 9. Molecular assembly of *meso–meso*-linked biporphyrin using crown-cation interaction.

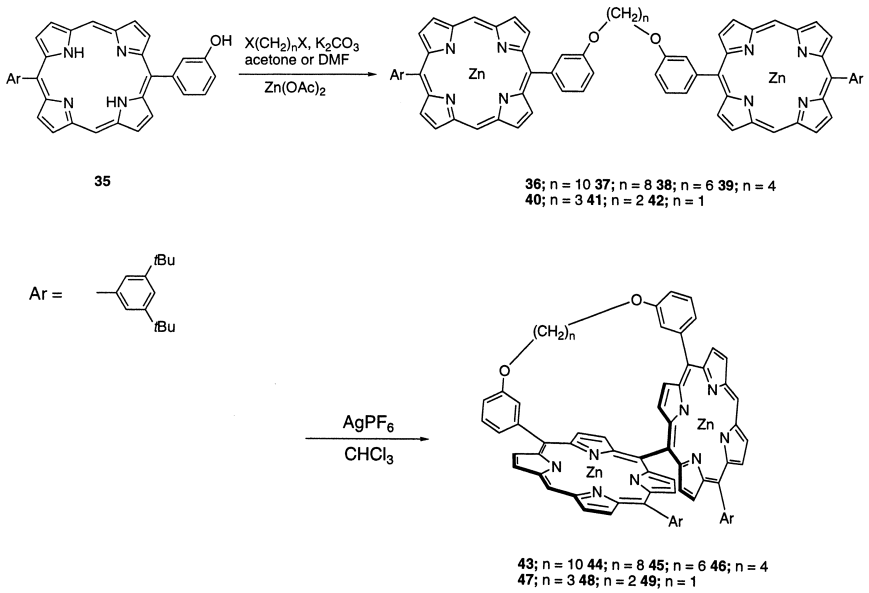

Scheme 10. Synthesis of strapped biporphyrins.

A divergent porphyrin assembling is also possible with crown-ether-appended *meso–meso*-linked biporphyrin **34** (Scheme 9).[49] In the presence of potassium ion, **34** forms a polymeric architecture different from *face-to-face* dimerization for the corresponding porphyrin monomer **33**. Addition of potassium ions to a solution of **33** in $CHCl_3$:MeCN (2:1) caused a construction of *face-to-face* porphyrin dimer, as reported for tetrakis(5,10,15,20-benzo-15-crown-5)porphyrin.[88] In contrast, addition of potassium ions to a solution of **34** led to linear extended aggregation (Scheme 9). The polymeric nature of the aggregate formed from **34** has been confirmed by light-scattering measurements, which indicated a molecular weight of approximately 1×10^5 daltons for the aggregate; that corresponds to an aggregation number of ca. 50.

3. Synthesis of Strapped *meso–meso*-Linked Biporphyrins

If the relative orientation of the two porphyrins in *meso–meso*-linked biporphyrin array could be changed in a systematic manner, it would constitute a nice set of models for a study on the effects of dihedral angle on the electronic coupling. Along this line, a series of strapped *meso–meso*-linked biporphyrins have recently been prepared.[48] Linearly bridged biporphyrins **36–42** were prepared by Williamson reaction of hydroxyphenylporphyrin **35** with corresponding dihaloalkane, followed by zinc insertion, in high yields (82–92%); strapped biporphyrins **43–49** were prepared through intramolecular Ag^I coupling reaction of **36–42** in highly-dilute conditions in moderate yields (20–60%), as shown in Scheme 10. MM2 calculations suggested a decrease in the dihedral angle with shortening of the strap, as expected. The absorption spectra of the strapped biporphyrins are very informative (Fig. 2). The absorption spectrum of **43** is quite similar to that of $\mathbf{Z_0}$**2**. The decrease of the strap length led to dramatic changes in the absorption spectra, as seen for **46** and **48**. In particular, the absorption spectrum of **48** exhibits four bands in the Soret band region, clearly reflecting a deviation from the orthogonal conformation. The one-electron oxidation potentials of **43–49** became increasingly lower with the decrease in the strap length,

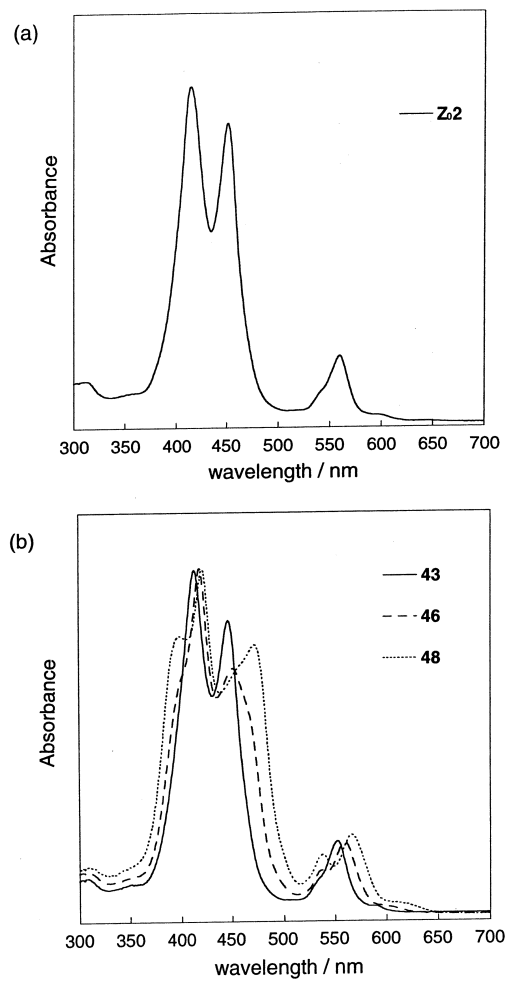

Fig. 2. UV-vis absorption spectra of (a) $\mathbf{Z_0}$**2**, and (b) **43** (n = 10), **46** (n = 4), and **48** (n = 2) in CH_2Cl_2.

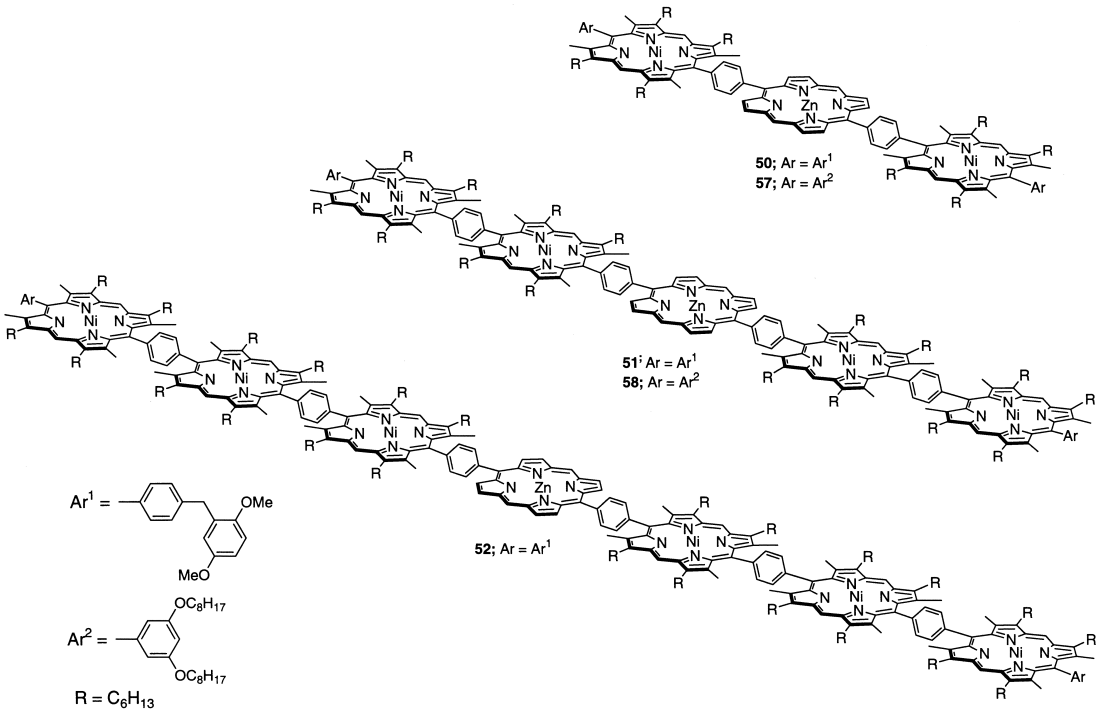

Chart 3. 1,4-Phenylene-bridged linear porphyrin arrays.

Table 1. The First Oxidation Potential (vs ferrocene/ferrocenium)
Calculated dihedral angles of **43**–**49** are given in parenthesis.

	E_{Oxl}/V		E_{Oxl}/V
43 (94°)	0.33	**36**	0.28
44 (90°)	0.32	**37**	0.27
45 (80°)	0.31	**38**	0.26
46 (71°)	0.30	**39**	0.30
47 (53°)	0.28	**40**	0.29
48 (42°)	0.27	**41**	0.29
49 (36°)	0.22	**42**	0.33

in accord with enhanced electronic communications between the two porphyrin rings (Table 1).

4. Application of *meso–meso* Coupling Reaction to Construction of Three-Dimensionally Arranged Windmill and Grid Porphyrin Arrays

In 1998, we reported the synthesis of windmill-like porphyrin arrays.[42] We soon extended this coupling reaction to the synthesis of three-dimensionally arranged grid-like porphyrin arrays.[43] These porphyrin arrays are of interest with a view to the construction of artificial light-harvesting antenna and molecular photonic wire, as well as an information storage molecular system.

4-1. Synthesis of Windmill Porphyrin Arrays. We examined the Ag^I-promoted coupling reaction of 1,4-phenylene-bridged linear porphyrin arrays such as trimer **50**, pentamer **51**, and heptamer **52** (Chart 3).[89–92] The reaction of the trimer **50** with two molar amounts of $AgPF_6$ produced porphyrin hexamer **53** along with porphyrin nonamer **54**, as monitored by analytical GPC/HPLC (Chart 4). The reaction was stopped after 22 h and **53** and **54** were isolated by recycling preparative GPC/HPLC in 50% and 2% yields, respectively, along with the recovery of **50** (47%). The orthogonal architecture of these arrays prevents π–π stacking and thus leads to the well-resolved ^{1}H NMR spectra, that reveal their symmetric structures. The coupling reaction of the linear pentamer **51** was similarly performed with three equivalents of $AgPF_6$ to give porphyrin decamer **55** in 35% isolated yield (Chart 5). Further, the reaction of the heptamer **52** with three molar amounts of $AgPF_6$ provided porphyrin tetradecamer **56** with a 14% isolated yield (Chart 6).

4-2. Synthesis of Grid Porphyrin Arrays. As indicated above, the coupling reaction of the linear porphyrin arrays often led to production of higher oligomerized porphyrin arrays such as the nonamer **54**. These results suggested that windmill porphyrins themselves could serve as effective building blocks for the Ag^I-promoted coupling reaction. Therefore, we examined Ag^I-promoted coupling reaction of the windmill porphyrin arrays. In these attempts, substrates **57** (porphyrin trimer) and **58** (porphyrin pentamer) bearing 3,5-dioctyloxyphenyl substituents as starting linear porphyrin arrays were employed in order to improve the solubilities of higher oligomeric porphyrin products. Windmill porphyrin hexamer **59** and windmill decamer **60** were prepared from porphyrin **57** and **58** in 22% and 28% yields, respectively. The reaction of **59** with two molar amounts of $AgPF_6$ for 9 h gave a mixture that contained porphyrin 12-mer, 18-mer, and 24-mer (Chart 7). These were isolated by recycling preparative GPC/HPLC to give the 12-mer **61** (25%) and small amounts of the 18-mer and the 24-mer along with the recovery of **59** (35%). Further, the grid porphyrin 12-mer **61** was coupled with 2.8 molar amounts of $AgPF_6$ under similar conditions to give higher oligomers. After 16 h,

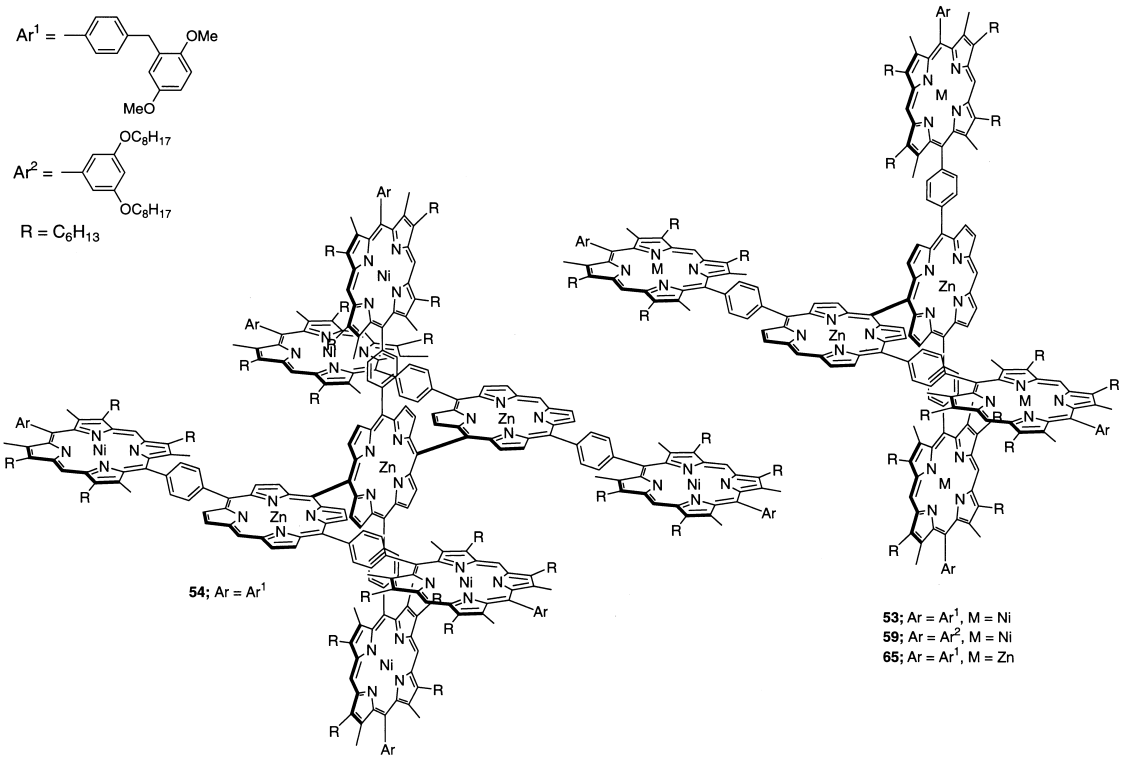

Chart 4. Windmill porphyrin arrays.

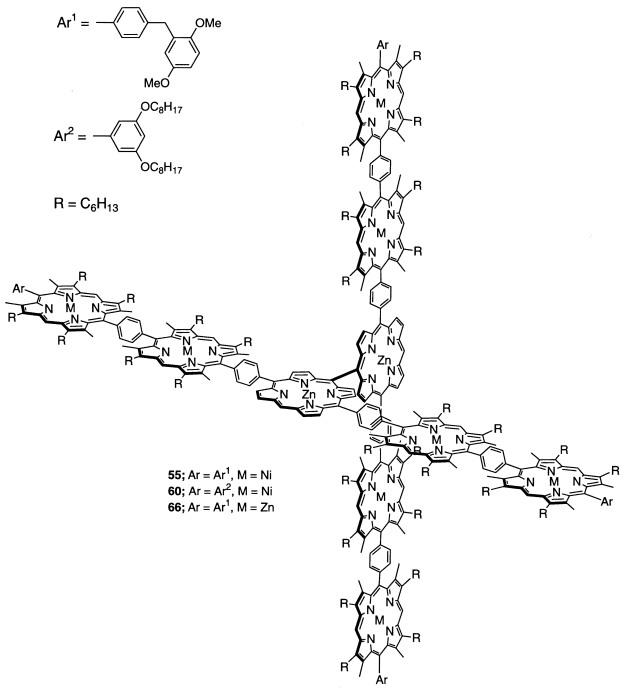

Chart 5. Decameric windmill porphyrin arrays.

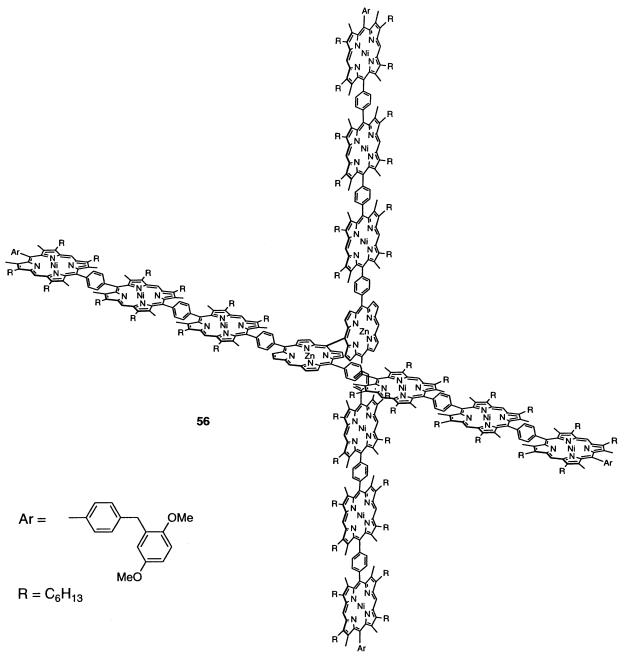

Chart 6. 14-Meric windmill porphyrin arrays.

products separated in a pure form displayed the parent ions at *m/z* 21466, 32276, and 43321, all in line with the expected grid porphyrin 24-mer **62** (calcd for $C_{1376}H_{1778}N_{96}Ni_{16}O_{32}Zn_8$: 21638), 36-mer **63** (calcd for $C_{2064}H_{2666}N_{144}Ni_{24}O_{48}Zn_{12}$: 32456) and 48-mer **64** (calcd for $C_{2752}H_{3554}N_{192}Ni_{32}O_{64}Zn_{16}$: 43274), respectively (Chart 7). The structure of the porphyrin 48-mer **64**, the largest grid array prepared, is shown in Chart 8.

4-3. Mechanistic Studies on Formation of Windmill Hexamer. The Ag^I-promoted coupling reaction of the 1,4-phenylene-bridged linear porphyrin arrays proceeded efficiently, giving the corresponding windmill porphyrin arrays with good yields and excellent *meso–meso* regioselectivity. Curiously, the coupling reactions of 1,4-phenylene trimers pro-

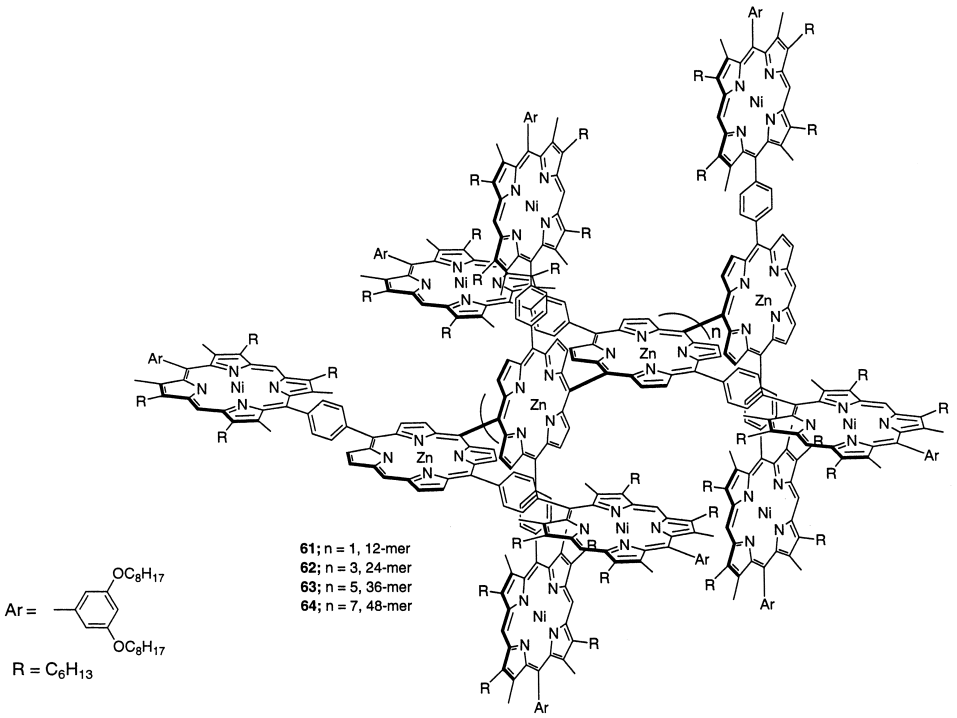

Chart 7. Grid-like porphyrin arrays.

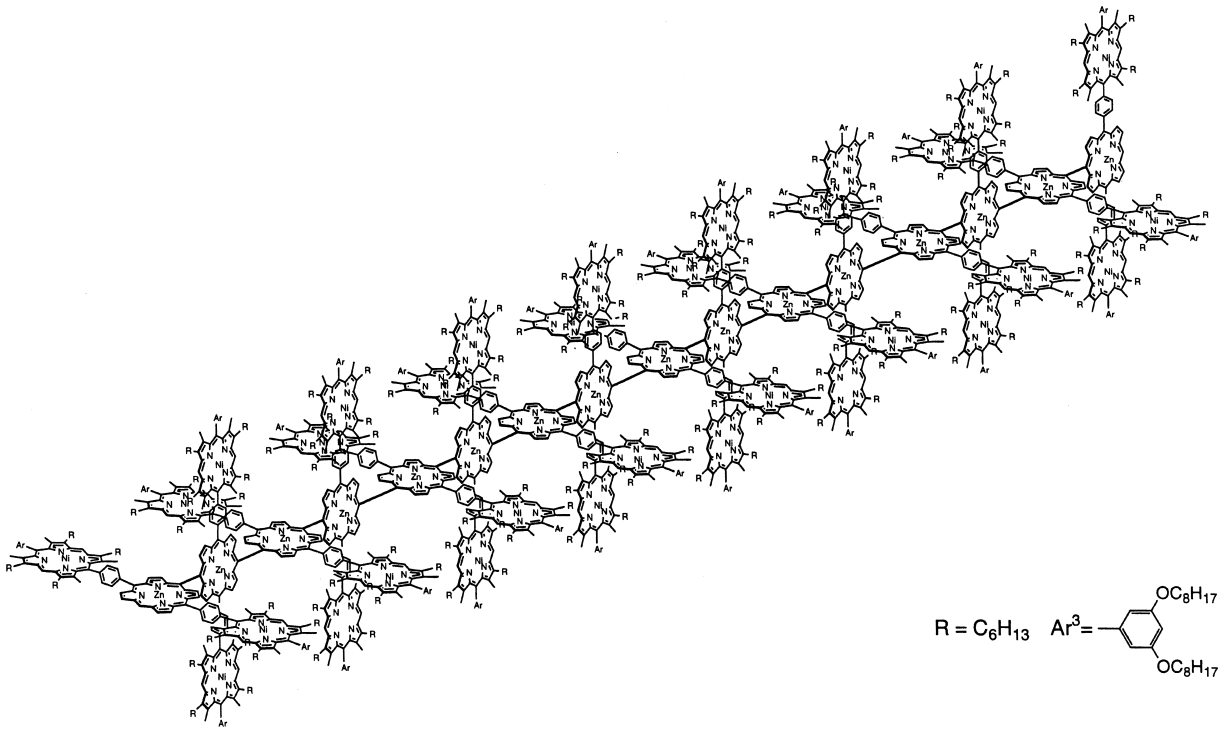

Chart 8. Structure of grid-like porphyrin 48-mer **64**.

ceeded at a similar rate or even faster in comparison to that of the parent porphyrin monomer. These results may be explained by a mechanism in which the peripheral Ni^{II} β-octaalkylporphyrins act as a mediator for the oxidation of the central Zn^{II} β-free porphyrin by Ag^{I} ions (Scheme 11). This mechanism was supported by the fact that the first one-electron oxidation potential of the central Zn^{II} β-free porphyrin (0.30 V) was similar to that of the peripheral Ni^{II} β-octaalkylporphyrins (0.32 V). Sterically, the peripheral Ni^{II} porphyrins should be much more accessible to the Ag^{I} ion. Namely, the initial oxidation of the peripheral Ni^{II} porphyrin by an Ag^{I} ion, followed by a hole transfer to the central Zn^{II} β-free porphyrin, was con-

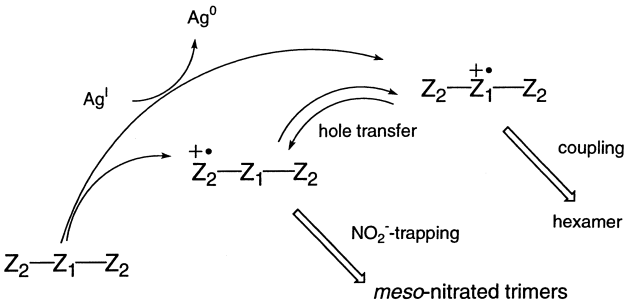

Scheme 11. Proposed mechanism of the Ag^{I}-promoted oxidative coupling reaction of porphyrin trimer Z_2–Z_1–Z_2.

sidered to assist generation of the radical cation of the central Zn^{II} β-free porphyrin. The results of competition experiments with other metallated porphyrin trimers and cation radical trapping experiments by $AgNO_2$ strongly supported this mechanism.

4-4. Intramolecular Singlet Excitation Energy Transfer in All Zinc(II) Windmill Porphyrin Arrays. Structurally well-defined architectures of these windmill and grid porphyrin arrays may be attractive for use in a variety of fields such as nano-scale optical and electrochemical molecular devices.[19–21] All the Zn^{II}-metallated windmill porphyrins allow an efficient singlet–singlet excitation energy transfer from the peripheral porphyrins to the central *meso–meso*-linked biporphyrin. In the steady-state fluorescence spectra, the fluorescence intensity of the peripheral porphyrins is reduced and that of the *meso–meso*-linked biporphyrin core is enhanced, indicating a singlet-singlet energy transfer reaction. The lower energy level of the S_1-state of the *meso–meso*-linked biporphyrin core (2.07 eV) relative to that of the peripheral porphyrins (2.13 eV) is responsible for this energy transfer. The time-resolved picosecond fluorescence spectra of **65** (Fig. 3) provided more support for the energy transfer, since the emission from the S_1-state of the peripheral porphyrins that predominated at an early stage decayed rapidly, and the broad emission from the S_1-state of the *meso–meso*-linked biporphyrin core was increased gradually following the energy transfer. Although the windmill arrays have energy transfer functions from the peripheral porphyrins to the biporphyrin core, the efficiency is not quantitative, mostly because of an insufficient energy gap between the energy donor and acceptor. Improvement of the energy transfer efficiency may be possible by a chemical modification at the *meso*-positions so as to place the energy level of the S_1-state of *meso–meso*-linked biporphyrin core sufficiently lower with respect to that of the peripheral porphyrin energy donors.[79,93,94]

5. An Approach Towards Unprecedented Giant Porphyrin Arrays with the Goal of the Longest Man-Made Molecule

As noted in the introduction part, the preparation and characterization of monodisperse giant molecules with precise structure and precise size have attracted considerable interest in light of their potential applications to the nascent field of molecular electronic devices. So far, the lengths of linear monodisperse π-conjugated oligomers have reached the range of ca. 10 nm.[14,17,89,95–100] Yet it still remains a great synthetic challenge to explore a discrete, finite functional supramolecule

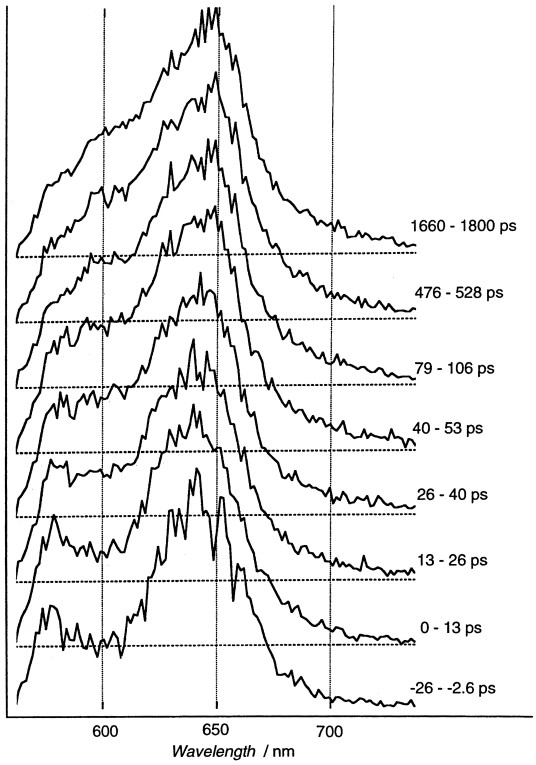

Fig. 3. Time-resolved fluorescence spectra of **65** in CH_2Cl_2 at room temperature for the excitation at 532 nm.

with a well-defined structure far beyond these achievements. In addition, achieving direct access to single molecules to bring information about them[20–27,101] has become a growing area of contemporary interdisciplinary research since the discovery of scanning tunneling microscopy (STM) at IBM's research laboratories in Zurich.[102] Research in this area has been directed toward the manipulation of single molecules[20] and the exploration of molecular properties on an individual nonstatistical basis.[21]

With these ideas in the background, we have launched a challenging project to repeat this *meso–meso* doubling reaction to make exceedingly long molecules until it ceases to work. Here it is appropriate to summarize again the advantages of this reaction: 1) the *meso–meso* coupling regioselectivity is quite high; 2) the porphyrin arrays have essentially the same linear rod-like shape; 3) the porphyrin arrays are highly soluble, presumably due to orthogonal conformations; 4) the separation of the coupling products is easy by recycling preparative GPC–HPLC chromatography as a result of large difference in molecular weight; and finally 5) the long coupling products still bear two free *meso*-positions available for the next reaction.

The long *meso–meso*-linked porphyrin arrays have the following properties: 1) on the basis of the linear molecular shape, the whole molecular length can be easily predicted by the number of porphyrins (8.35 Å per one porphyrin unit); 2) the large Coulombic interactions between the neighboring porphyrins are favorable for rapid excitation-energy transmissions; 3) each porphyrin unit retains its individual character, presumably due to the orthogonal geometry, thus minimizing

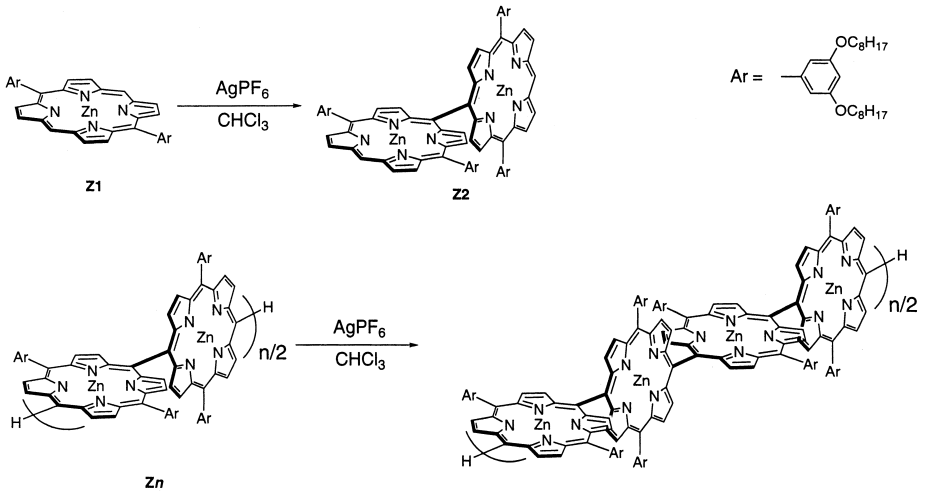

Scheme 12. Ag^{I}-promoted doubling reaction of Zn^{II} 5,15-diarylporphyrin and *meso–meso*-linked porphyrin arrays.

formation of any stacked energy sink which will disrupt the energy flow along the arrays. In other word, *meso–meso*-linked porphyrin arrays are expected to realize the fast and high-efficient energy transfer over a long distance down the array and thus can be utilized as good candidates for energy transfer functional arrays in molecular photonic devices.[103,104]

5-1. Synthesis. Initially we employed Zn^{II} bis(3,5-di-*t*-butylphenyl)porphyrin as a building block element, but we encountered a serious solubility problem at the stage of $\mathbf{Z_0 8}$. In order to circumvent the solubility problem, more soluble Zn^{II} bis(3,5-dioctyloxylphenyl)porphyrin **Z1** (we denote the dioctyloxyphenyl substituted *meso–meso*-linked Zn^{II}-porphyrin arrays as **Z*n***, where *n* represents the number of the porphyrins) was employed, which was readily prepared from 3,5-dioctyloxybenzaldehyde and dipyrromethane in 36% yield under the standard conditions.[73,74] 3,5-Dioctyloxybenzaldehyde was isolated in 65% total yield (4 steps) from 3,5-dihydroxybenzoic acid. Chain elongation strategy of porphyrin arrays is quite simple by repeating the dimerization reactions from **Z1** to **Z2**, **Z2** to **Z4**, **Z4** to **Z8**, **Z8** to **Z16**, and **Z16** to **Z32** (Scheme 12). The reaction of **Z1** with 1.2 mol amt. of $AgPF_6$ at 30 °C in $CHCl_3$ for 10 h, followed by preparative SEC, gave **Z2** in 20–24% yield, **Z3** in 3–6% yield, and high oligomers, along with recovery of **Z1** (60–65%). In an essentially similar manner, yields of the other dimerization products were commonly 20–30% along with the recovery of starting materials (55–60%). Finally the coupling reaction of **Z32** afforded **Z64**, **Z96**, and **Z128**. The longest porphyrin array **Z128** isolated from the reaction of **Z32** was identical with the dimerization product obtained from the reaction of **Z64**. During these repeated preparations, we also isolated **Z3**, **Z5**, **Z6**, **Z7**, **Z10**, **Z12**, **Z20**, **Z24**, **Z40**, and **Z48**. Use of pure $CHCl_3$ as the solvent and strict control of the reaction temperature at 30 °C were crucial in order to avoid polymerization of Zn^{II} porphyrin. Also equally important was the use of recycling GPC/HPLC for product separation. Figure 4 shows GPC/HPLC chromatographs of the reactions of **Z16** and **Z32**. The coupling products were nicely separated over the GPC/HPLC in both cases, owing to large differences in molecular weights. The molecular weights determined by MALDI-TOF MS method and the retention time of these porphyrin arrays are given in Table 2.[45]

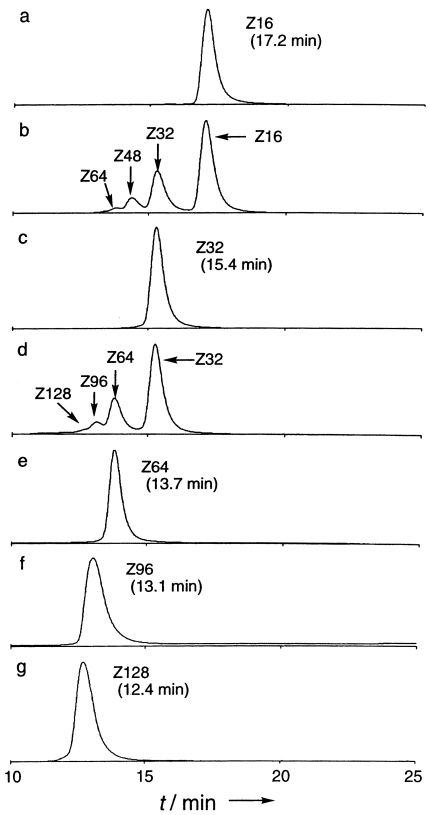

Fig. 4. GPC–HPLC chromatograms of the Ag^{I}-promoted coupling reaction detected at 413 nm. Each chromatogram is normalized to the maximum intensity. The reaction of **Z16** (a–c) and **Z32** (c–g): (a) **Z16**, (b) after 9 h, (c) purified **Z32**, (d) after 9 h, (e) purified **Z64**, (f) purified **Z96**, and (g) purified **Z128**.

To our surprise, the longer arrays **Z64** and **Z128** display relatively well-resolved ^1H NMR spectra, like those of the shorter arrays. It is noteworthy that the *meso*-protons, outer β-protons, and many inner β-protons appear at nearly the same chemical shifts for all the arrays, indicating no significant aggregation of the arrays under these conditions.

Additionally, all these Zn^{II} porphyrin arrays also were con-

Table 2. Molecular Weights and Retention Times of the Porphyrin Arrays

Compound	Molecular formula	Mc[a)]	Mo[b)]	Retention time[c)]
				min
Z1	$C_{64}H_{84}N_4O_4Zn$	1037	1036	22.4
Z2	$C_{128}H_{166}N_8O_8Zn_2$	2075	2076	21.4
Z3	$C_{192}H_{248}N_{12}O_{12}Zn_3$	3114	3112	20.7
Z4	$C_{256}H_{330}N_{16}O_{16}Zn_4$	4146	4145	20.3
Z5	$C_{320}H_{412}N_{20}O_{20}Zn_5$	5186	5183	19.9
Z6	$C_{384}H_{494}N_{24}O_{24}Zn_6$	6222	6214	19.4
Z7	$C_{448}H_{576}N_{28}O_{28}Zn_7$	7259	7253	19.1
Z8	$C_{512}H_{658}N_{32}O_{32}Zn_8$	8296	8286	18.8
Z10	$C_{640}H_{822}N_{40}O_{40}Zn_{10}$	10369	10351	18.3
Z12	$C_{768}H_{986}N_{48}O_{48}Zn_{12}$	12443	12416	17.9
Z16	$C_{1024}H_{1314}N_{64}O_{64}Zn_{16}$	16590	16566	17.2
Z20	$C_{1280}H_{1642}N_{80}O_{80}Zn_{20}$	20736	20679	16.6
Z24	$C_{1536}H_{1970}N_{96}O_{96}Zn_{24}$	24884	24465	16.0
Z32	$C_{2048}H_{2626}N_{128}O_{128}Zn_{32}$	33178	33292	15.4
Z40	$C_{2560}H_{3282}N_{160}O_{160}Zn_{40}$	41470	41177	14.8
Z48	$C_{3072}H_{3938}N_{192}O_{192}Zn_{48}$	49764	49497	14.3
Z64	$C_{4096}H_{5250}N_{256}O_{256}Zn_{64}$	66350	66323	13.7
Z96	$C_{6144}H_{7874}N_{384}O_{384}Zn_{96}$	99527	99050	13.1
Z128	$C_{8192}H_{10498}N_{512}O_{512}Zn_{128}$	132709	130295	12.4

a) Calculated molecular weight. b) MALDI-TOF mass detected molecular weight.
c) GPC–HPLC analysis (JAIGEL-2.5H-AF, 3H-AF and 4H-AF columns in series).

verted into the corresponding free-base porphyrin in good yields that were subsequently metallated with a variety of metal ions to give the metalled *meso–meso*-linked arrays (Cu^{II}, Ni^{II}, and Pd^{II} etc.). The free-base porphyrin arrays exhibited ^{1}H NMR spectra quite similar to those of the Zn^{II}-porphyrin arrays. Interestingly, the inner-NH signals appeared at different chemical shifts, reflecting the influence of the ring current effect of neighboring porphyrins, at higher field for the outer porphyrin and at lower field for the inner porphyrins.

5-2. Systematic Photophysical Studies on Absorption Spectra of *meso–meso*-Linked Porphyrin Arrays. The absorption spectra normalized at ca. 413 nm are shown in Fig. 5. As reported previously,[38–59] the *meso–meso*-coupled porphyrin arrays exhibit large splitting of Soret bands due to strong exciton coupling.[83] With increase in the number of porphyrins, the low-energy Soret band is shifted to longer wavelength, while the high-energy Soret band remains at nearly the same wavelength (413–414 nm), resulting in a progressive increase in the splitting energy. The intensity of longer wavelength bands of Soret bands becomes increasingly stronger relative to that of the high energy Soret bands and the spectral shifts in the Q band region are modest, with gradual increase in intensity.

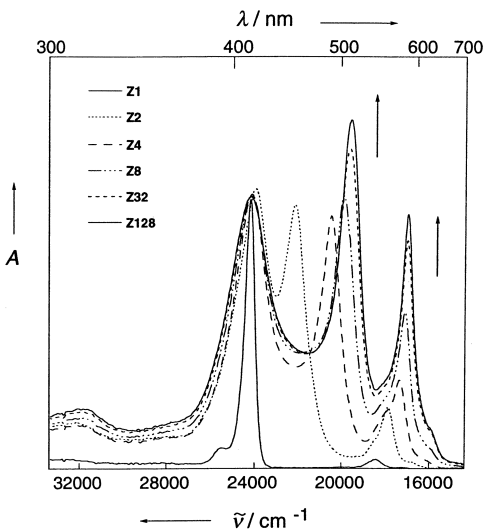

Fig. 5. Absorption spectra of **Z1**, **Z2**, **Z4**, Z8, **Z32**, and **Z128** taken in THF.

The systematic spectral changes can be explained by the simple point-dipole exciton coupling theory developed by Kasha.[81] The Soret band of a Zn^{II}-porphyrin has two perpendicular components: B_X and B_Y. A schematic energy level diagram is shown in Scheme 13. In simple monomer, they are approximately degenerate (E_u in D_{4h}), but in porphyrin dimer they couple differently. In the case of **Z2**, only B_X transitions along the *meso–meso* bond are in line, inducing the dipole–dipole interaction and only the in-phase perturbation gives the allowed exciton states, resulting in a red-shift, while the other dipole interactions should be canceled due to the perpendicular conformation between neighboring porphyrins. Unperturbed Soret transitions at 413–414 nm for all the arrays suggest the averaged perpendicular conformation vice versa. These interpretations coincide with the observed spectra of these arrays and indicate that the adjacent porphyrin rings have an orthogonal geometry in solution. The X-ray crystallography[55,84] in the solid state and AM1 calculations[41] also suggest the orthogonal geometry.

The Coulombic interaction energy (E) depends on the magnitude of the transition dipole moments as well as the distance, as written by Eq. 1:

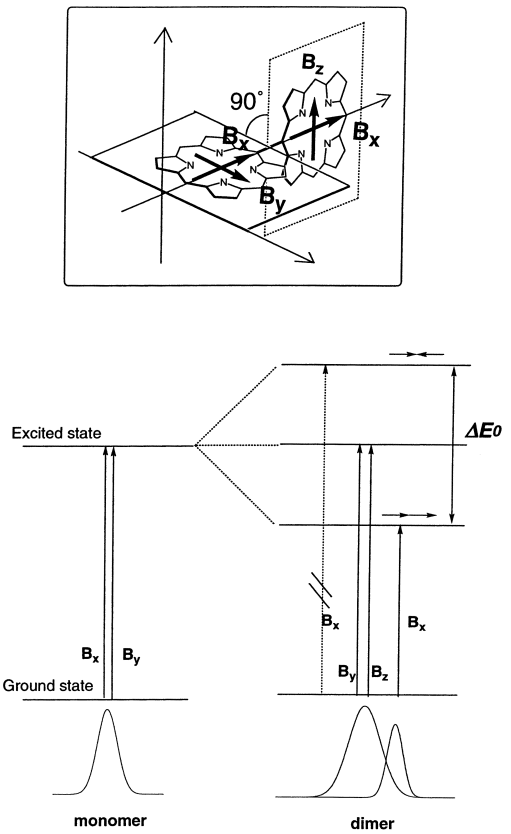

Scheme 13. Schematic energy level diagram for *meso–meso*-linked Zn^{II}-biporphyrin.

$$E = \frac{1}{4\pi\varepsilon_0}\left[\frac{\mu_1 \cdot \mu_2}{R^3} - 3\frac{(\mu_1 \cdot r)(\mu_2 \cdot r)}{R^5}\right] \quad (1)$$

Here μ_i is the transition dipole moment of molecule i, r is the position vector linking the centers of two molecules, and R is the center-to-center chromophore distance. When two dipoles are parallel, E is expressed by

$$E = \frac{|\mu_1||\mu_2|}{4\pi\varepsilon_0 R^3}(1 - 3\cos^2\theta) \quad (2)$$

Where θ is the angle between the polarization axes and the line of molecular centers. In the case of *meso–meso*-linked linear porphyrin dimer ($\theta = 0$, $\mu_1 = \mu_2 = \mu$), therefore, exciton splitting energy corresponding to the separation $\Delta E_0 = 2E$ is given by Eq. 3.[81]

$$\Delta E_0 = \frac{\mu^2}{\pi\varepsilon_0 R^3} \quad (3)$$

The exciton band width (ΔE) for larger linear arrays should be given by Eq. 4, when the excitonic interactions between non-nearest neighbor porphyrins are negligible owing to longer distance.

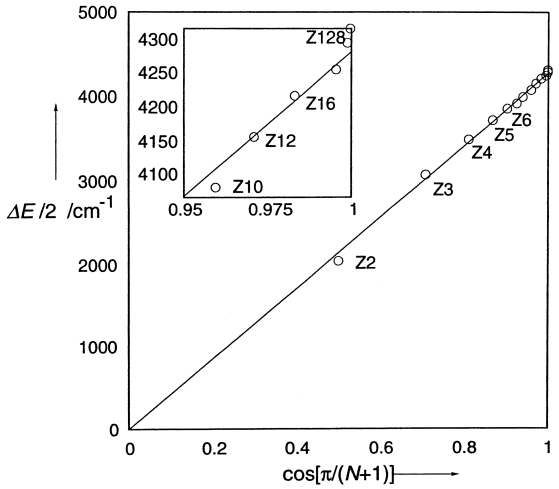

Fig. 6. Plot of ΔE versus $2\cos[(\pi/(N+1)]$.

$$\Delta E = 2\,\Delta E_0 \cos[\pi/(N+1)] \quad (4)$$

Here N represents the number of chromophores. The exact value of ΔE is not known because the transition to the highest energy excitonic state is forbidden. Therefore, the splitting energy ΔE can be taken to be twice the value of the difference in energy between the red-shifted B_X band and the unperturbed $B_{Y,Z}$ band. When ΔE data were plotted to Eq. 4, a nicely straight line with a slope of $\Delta E_0 = 4250\ cm^{-1}$ was obtained (Fig. 6). The observed linear relationship indicates that the absorption spectral shapes are actually influenced by the number of porphyrins and the constituent porphyrins are regularly aligned in the same linear arrangement in the solution. On this basis, these arrays in the ground state are believed to consist of repeating individual chromophores with substantial electronic interactions.

The exciton delocalization length (coherent length) has been a central issue in the natural light harvesting systems[105–107] as well as J-aggregates of synthetic pigments.[108] We thus attempted to estimate the coherent length for these arrays on the basis of the fluorescence properties. The steady-state fluorescence spectra of the arrays are shown in Fig. 7. The monomer **Z1** exhibits two-peak emission (584 and 633 nm) characteristic of Zn^{II} porphyrin and the dimer **Z2** displays a red-shifted and broader fluorescence spectrum. The fluorescence spectra of the larger arrays (**Z3**–**Z128**) are observed in nearly the same region, with two bands at ca. 15600 cm^{-1} (640 nm) and ca. 15000 cm^{-1} (667 nm). The relative intensities of these two fluorescence bands are plotted against the number of porphyrins (Fig. 8). The fluorescence quantum yields determined with respect to $\Phi_F = 0.03$ of ZnTPP[109] increase up to **Z16**, but then decrease with the increase of the number of porphyrins. With the fluorescence lifetimes (τ_F) obtained by time-correlated single-photon counting technique, the natural radiative rates (k_F) have been calculated according to Eq. 5:

$$k_F = \Phi_F/\tau_F \quad (5)$$

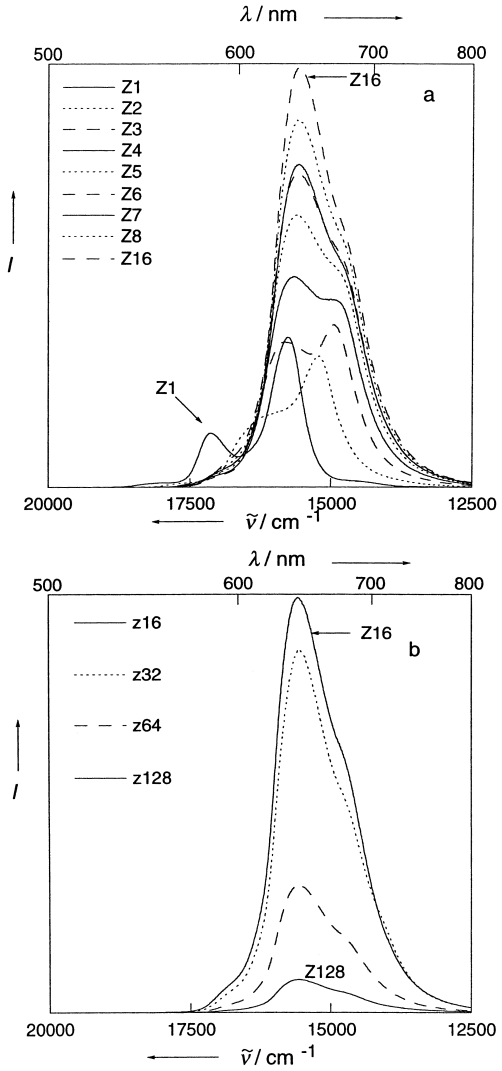

Fig. 7. The fluorescence spectra of the porphyrin arrays taken after excitation of a THF solution at 413 nm with the absorbance at 413 nm adjusted at 0.20. (a) **Z1**–**Z8** and **Z16**, (b) **Z16**, **Z32**, **Z64**, and **Z128**.

The fluorescence decays of shorter arrays obey a single exponential function, but those of longer arrays (**Z32**, **Z64**, and **Z128**) can be fit only with a biexponential function and thus we used the averaged lifetimes. Figure 8 also shows the plots of the inverse of k_F versus the number of porphyrins. It is now apparent that the radiative rate increases steadily from **Z1** to **Z6**–**Z8** and becomes rather constant for the arrays larger than **Z6**–**Z8**. The plot of the relative fluorescence intensity also reveals a similar trend, indicating that the fluorescence shape becomes rather constant at **Z6**–**Z8**. On the basis of these results, the coherent length has been estimated to be 6–8, over which the exciton is delocalized. Comparison of the coherent length in these artificial system with that in the natural antenna systems such as LH1 and LH2 would be interesting.

6. Synthesis of Fused Porphyrin Arrays

In recent years, the creation of electronically π-conjugated porphyrin arrays in which the porphyrin π-electronic systems merge to form large supramolecular chromophores is an attractive target by virture of their remarkable photophysical and electrochemical properties. Such conjugated porphyrin arrays are thus of interest in view of their potential for use as a conducting electronic wire. The central issue is definitely to increase the electronic interaction between the constituent porphyrins in the arrays. The degree of electronic interactions can be evaluated from red-shifted absorption band arising from the decreased optical HOMO–LUMO gap. Two important classes of π-conjugated porphyrin arrays which have recently been explored: 1) *meso*-ethyne-linked and *meso*-butadiyne-linked Zn^{II}-porphyrin and their oligomeric analogs,[31] and 2) fused porphyrin arrays where the individual porphyrin rings are bridged by coplanar aromatic spacers.[29] In the latter case, the porphyrin units are forced to take an overall coplanar geometry, giving rise to full conjugation over the array. As a pioneering work, Crossley et el. have employed the condensation of porphyrin-2,3-diones and porphyrin-2,3,12,13-tetraones with aromatic *ortho*-diamines and 1,2,4,5-tetraamines for the construction of the planar fused porphyrin array bridged by 1,4,5,8-tetraazaanthracene spacer.[110–112] They have extended this strategy up to a tetra-porphyrin array with 65 Å molecular length. A benzene-bridged fused dibenzoporphyrin synthesized by Kobayashi et al. reported to display the absorption band at 711 nm, also indicating its conjugated character.[113] A set of directly fused porphyrin arrays have been developed by Smith et al., where pyrroloporphyrin precursers play a central role.[114–117] They have extended this strategy to the synthesis of cross-shaped fused pentakis porphyrin arrays.[117]

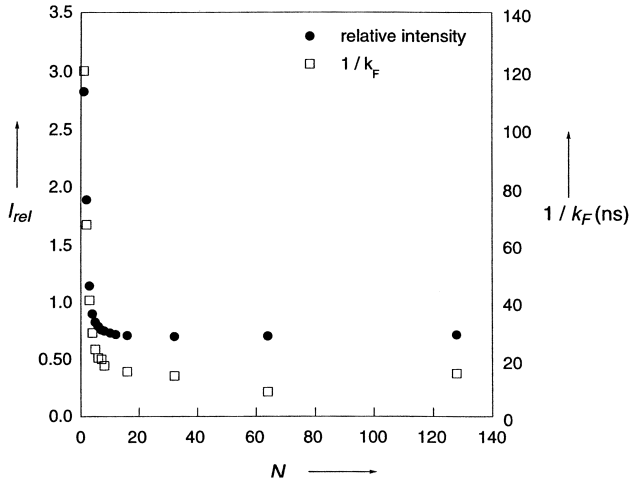

Fig. 8. Plots of the inverse of k_F (□) and the relative fluorescence intensity (●) of two peaks versus the number of porphyrins (*N*).

In the course of our studies on the *meso–meso* coupling reactions, we found that treatment of 5,10,15-triarylsubstituted Ni^{II}-porphyrin **67** with tris(4-bromophenyl)aminium hexachloroantimonate $(p\text{-}BrC_6H_4)_3NSbCl_6$ (BAHA) in $CHCl_3$ for 12 h led to the formation of *meso–β* doubly-linked biporphyrins **68** in 53% yield.[70] Further we found that oxidation of *meso–meso*-linked Cu^{II}-biporphyrin **69** with BAHA in C_6F_6 led to the formation of *meso–meso β–β β–β* triply-linked biporphyrins **70** (Scheme 14).[72] In this reaction, C_6F_6 is a better solvent for suppressing *β*-chlorination. X-ray crystallography revealed the structures of **68** and **70**, in which the fused biporphyrins

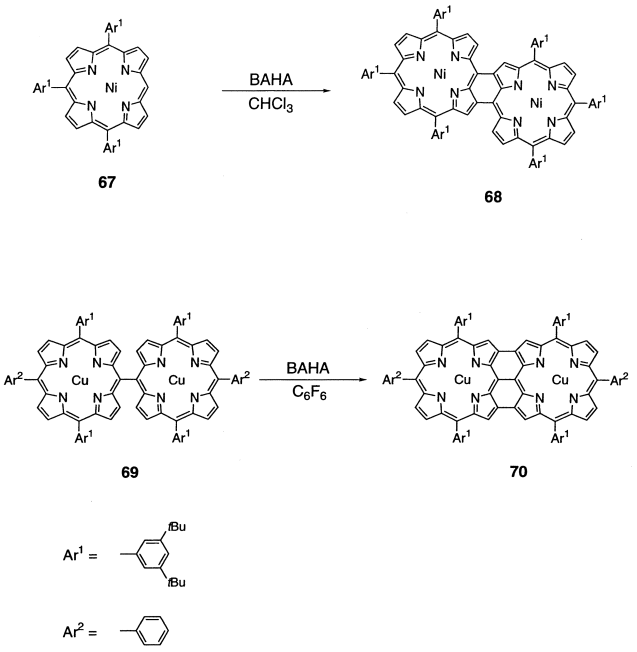

Scheme 14. Synthetic scheme of fused porphyrin.

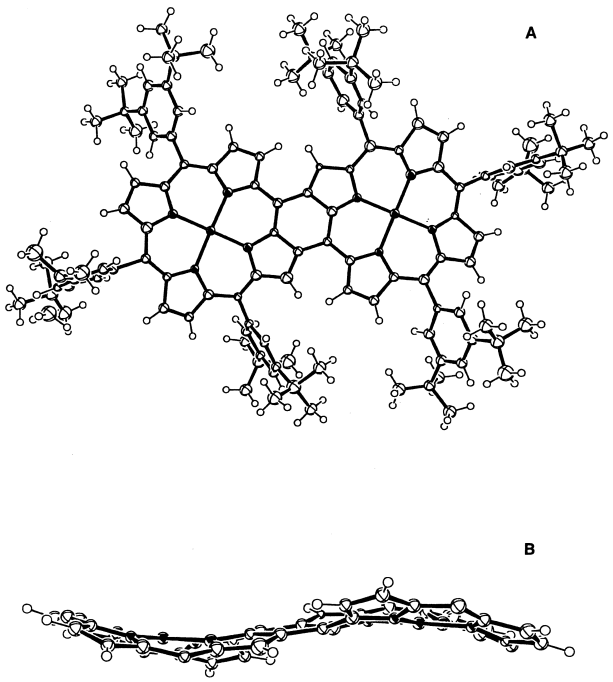

Fig. 9. Molecular structure of **68**. (A) Top view, (B) side view. Hydrogen atoms and solvent molecules are omitted for clarity.

adopt highly planar structures. The two Ni^{II}-porphyrin rings in **68** adopt a ruffled conformation (Fig. 9) while the Cu^{II}-porphyrins are almost completely flat in **70** (Fig. 10). The newly formed *meso–β* bonds in **68** are 1.45 Å long, and *meso–meso* and *β–β* bonds in **70** are 1.44 and 1.41 Å long, respectively. In addition, the remarkably red-shifted absorption spectra of fused biporphyrins (with λ_{max} at 756 nm for **68** and 996 nm for **70**) indicate the fully delocalized π-conjugated character. The

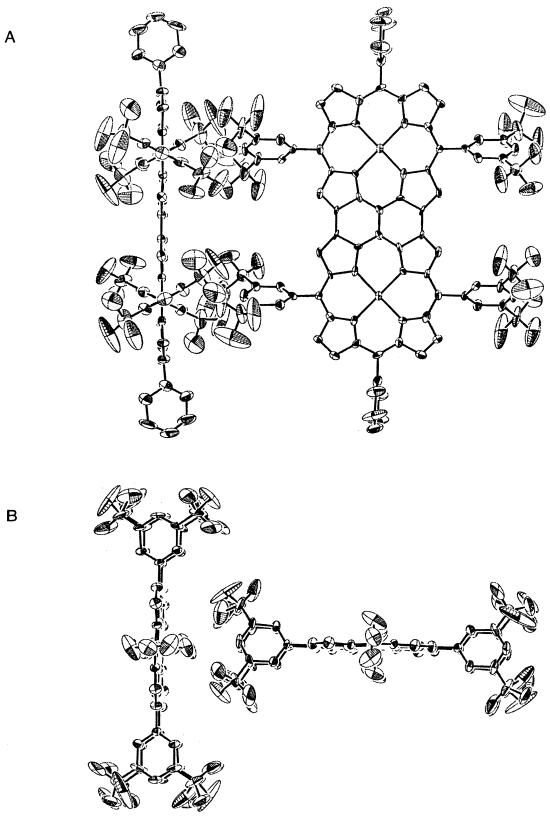

Fig. 10. Molecular structure of **70**. (A) Top view, (B) side view. Hydrogen atoms and solvent molecules are omitted for clarity.

delocalized π-conjugations over the array were also suggested from their electrochemical properties. In light of the strong donor ability with extremely small HOMO–LUMO gap, which are evinced from the lowered one-electron oxidation potentials and the red-shifted intense absorption bands,[72] the directly fused oligoporphyrin arrays are very promising for use as nonlinear optical materials and molecular motif in nano-scale molecular technology.

7. Conclusion and Future Work

The Ag^I-promoted oligomerization of *β*-free 5,15-diarylporphyrins led to an efficient construction of one, two, and three-dimensionally arranged porphyrin arrays. The coupling proceeded regioselectively only at the *meso*-position of Zn^{II} *β*-free arylporphyrin. These multi-porphyrin arrays have the following advantageous characteristics: 1) good solubility in various organic solvents in spite of large molecular size; 2) easy extension to higher arrays; 3) easy separation over the recycling preparative GPC/HPLC; and 4) controlled and regular inter-porphyrin distances and angles and thus constant and large inter-porphyrin electronic interactions that enable the efficient excitation energy hopping.

During the past decade, π-conjugated oligomers investigated as advanced materials for electronic and photonic applications have attracted ever-increasing interest from both academic and industrial researchers. A second interest of π-conjugated oligomers arises from their potential to act as molecular wires in molecular scale electronics and nanotechnological de-

vices.[16–19] In recent years, interdisciplinary groups of chemists, physicists, and engineers have performed a series of demonstrations by showing that individual or small packets of molecules, mounted within addressable scaffolds, can conduct electrical currents.[24,25] In the 20th century, many kinds of electronic devices based on polymers and oligomers were developed, and hereafter many kinds of electronic devices based on single molecule may appear.[18,21] In addition, the 21st century also will be a photonic century in which we use *light*, rather than *electrons*, as the medium for carrying information since light-based devices have potential advantages in comparison with ordinary designs.[28] Directly linked porphyrin arrays may serve as a potential photonic wire that is capable of transmitting excitation energy over long distance as results of favorable features, including a linear rod-like shape, ample Coulombic interactions for rapid coherent/incoherent energy transfer, and a lack of an energy sink that disrupts the energy flow along the arrays. These properties originate from the orthogonal conformation of the arrays, which tends to minimize the electronic interactions between the neighboring porphyrins.

Triply linked fused porphyrins made from *meso–meso*-linked porphyrins exhibit properties associated with an extremely delocalized π-electronic system as a consequence of their planar structure, enforced by the fused connections. This promising reaction strongly encourages the creation of a perfect molecular wire in which an electron can be transmitted rather freely from end to end. Extension of this synthetic strategy to higher oligomeric and polymeric porphyrin arrays is a fascinating next project that is actively in progress in our laboratory.[118]

The authors thank collaborators of our group at Kyoto University for their contributions to this work. We are grateful to Professor I. Yamazaki, Dr. T. Yamazaki, and Dr. Y. Nishimura at Hokkaido University for the fluorescence measurements and also to Professor D. Kim and his collaborators at KRISS and Yonsei University for the measurements on a variety of photophysical properties of the *meso–meso*-linked porphyrin arrays.

References

1 J. Deisenhofer, O. Epp, K. Miki, R. Huber, and H. Michel, *J. Biol. Chem.*, **180**, 385 (1984).

2 N. Krauss, W. Hinrichs, I. Witt, P. Fromme, W. Pritzkow, Z. Dauter, C. Betzel, K. S. Wilson, H. T. Witt, and W. Saenger, *Nature*, **361**, 326 (1993).

3 G. McDermott, S. M. Prince, A. A. Freer, A. M. Hawthornthwaite-Lawless, M. Z. Papiz, R. J. Cogdell, and N. W. Isaacs, *Nature*, **374**, 517 (1995).

4 R. E. Fenna and B. W. Matthews, *Nature*, **258**, 573 (1975).

5 J. Koepke, X. Hu, C. Muenke, K. Schulten, and H. Michel, *Structure*, **4**, 581 (1996).

6 S. Karrasch, P. Bullough, and R. Ghosh, *EMBO J.*, **14**, 631 (1995).

7 M. R. Wasielewski, *Chem. Rev.*, **92**, 435 (1992).

8 D. Gust, T. A. Moore, and A. L. Moore, *Acc. Chem. Res.*, **26**, 198 (1993).

9 J. Wojaczynski and L. Lotos-Grazynski, *Coord. Chem. Rev.*, **204**, 113 (2000).

10 H. Shinmori and A. Osuka, *J. Synth. Org. Chem. Jpn.*, **57**, 749 (1999).

11 T. Imamura and K. Fukushima, *Coord. Chem. Rev.*, **198**, 133 (2000).

12 J. P. Collman, P. Denisevich, M. Marocco, C. Koval, and F. C. Anson, *J. Am. Chem. Soc.*, **102**, 6027 (1980).

13 R. E. Martin and F. Diederich, *Angew. Chem., Int. Ed.*, **38**, 1350 (1999).

14 R. E. Martin, U. Gubler, J. Cornil, M. Balakina, C. Boudon, C. Bosshard, J.-P. Gisselbrecht, F. Diederich, P. Günter, M. Gross, and J.-L. Bredas, *Chem. Eur. J.*, **6**, 3622 (2000).

15 P. F. H. Schwab, M. D. Levin, and J. Michl, *Chem. Rev.*, **99**, 1863 (1999).

16 J. M. Tour, *Chem. Rev.*, **96**, 537 (1996).

17 J. M. Tour, *Acc. Chem. Rev.*, **33**, 791 (2000).

18 M. A. Reed and J. M. Tour, *Sci. Am.*, **282**, 86 (2000).

19 A. Aviram and M. Ratner, *Chem. Phys. Lett.*, **29**, 277 (1974).

20 Single Molecules Special Issue, *Science*, **283**,1667 (1999).

21 C. Joachim, J. K. Gimzewski, and A. Aviram, *Nature*, **408**, 541 (2000).

22 T. A. Jung, R. R. Schlittler, J. K. Gimzewski, H. Tang, and C. Joachim, *Science*, **271**, 181 (1996).

23 S.-W. Hla, L. Bartels, G. Meyer, and K.-H. Rieder, *Phys. Rev. Lett.*, **85**, 2777 (2000).

24 D. Porath, A. Bezryadin, S. de Vries, and C. Dekker, *Nature*, **403**, 635 (2000).

25 J. Chen, M. A. Reed, A. M. Rawlett, and J. M. Tour, *Science*, **286**, 1550 (1999).

26 M. T. Cygan, T. D. Dunbar, J. J. Arnold, L. A. Bumm, N. F. Shedlock, T. P. Burgin, L. II Jones, D. L. Allara, J. M. Tour, and P. S. Weiss, *J. Am. Chem. Soc.*, **120**, 2721 (1998).

27 M. A. Reed, C. Zhou, C. J. Muller, T. P. Burgin, and J. M. Tour, *Science*, **278**, 252 (1997).

28 I. Yamazaki, A. Osuka, and N. Ohta, *Mol. Cryst. Liq. Cryst.*, **315**, 235 (1998).

29 M. G. H. Vicente, L. Jaquinod, and K. M. Smith, *Chem. Commun.*, **1991**, 1771.

30 J.-H. Chou, M. E. Kosal, N H. Nalwa, S. A. Rakow, and K. S. Suslick, in "The Porphyrin Handbook," ed by K. Kadish, K. M. Smith, and R. Guilard, Academic Press, New York (1999), Vol. 6, p. 43.

31 H. L. Anderson, *Chem. Commun.*, **1999**, 2323.

32 V. S.-Y. Lin, S. G. DiMagno, and M. J. Therien, *Science*, **264**, 1105 (1994).

33 D. P. Arnold and L. Nitschinsk, *Tetrahedron Lett.*, **34**, 693 (1993).

34 H. L. Anderson, *Inorg. Chem.*, **33**, 972 (1994).

35 A. K. Burrell, D. Officer, and D. Reid, *Angew. Chem., Int. Ed. Engl.*, **34**, 900 (1995).

36 A. Osuka, B.-L. Liu, and K. Maruyama, *Chem. Lett.*, **1993**, 949.

37 J. J. Piet, P. N. Taylor, H. L. Anderson, A. Osuka, and J. M. Warman, *J. Am. Chem. Soc.*, **122**, 1749 (2000).

38 A. Osuka and H. Shimidzu, *Angew. Chem., Int. Ed. Engl.*, **36**, 135 (1997).

39 M. Terazima, H. Shimidzu, and A. Osuka, *J. Appl. Phys.*, **81**, 2946 (1997).

40 N. Yoshida, H. Shimidzu, and A. Osuka, *Chem. Lett.*, **1998**, 55.

41 H. S. Cho, N. W. Song, Y. H. Kim, S. C. Jeoung, S. Hahn, D. Kim, S. K. Kim, N. Yoshida, and A. Osuka, *J. Phys. Chem. A*, **104**, 3287 (2000).

42 A. Nakano, A. Osuka, I. Yamazaki, T. Yamazaki, and Y. Nishimura, *Angew. Chem., Int. Ed.*, **37**, 3023 (1998).
43 A. Nakano, T. Yamazaki, Y. Nishimura, I. Yamazaki, and A. Osuka, *Chem. Eur. J.*, **6**, 3254 (2000).
44 N. Yoshida, N. Aratani, and A. Osuka, *Chem. Commun.*, **2000**, 197.
45 N. Aratani, A. Osuka, Y. H. Kim, D. H. Jeong, and D. Kim, *Angew. Chem., Int. Ed.*, **39**, 1458 (2000).
46 Y. H. Kim, D. H. Jeong, D. Kim, S. C. Jeoung, H. S. Cho, S. K. Kim, N. Aratani, and A. Osuka, *J. Am. Chem. Soc.*, **123**, 76 (2001).
47 N. Yoshida and A. Osuka, *Tetrahedron Lett.*, **41**, 9287 (2000).
48 N. Yoshida and A. Osuka, *Org. Lett.*, **2**, 2963 (2000).
49 H. Shinmori and A. Osuka, *Tetrahedron Lett.*, **41**, 8527 (2000).
50 M. Ikeda, S. Shinkai and A. Osuka, *Chem. Commun.*, **2000**, 1047.
51 T. Ogawa, Y. Nishimoto, N. Yoshida, N. Ono, and A. Osuka, *Angew. Chem., Int. Ed.*, **38**, 176 (1999).
52 T. Ogawa, Y. Nishimoto, N. Yoshida, N. Ono, and A. Osuka, *Chem. Commun.*, **1998**, 337.
53 Synthesis of *meso–meso*-linked porphyrin dimers and trimers by other nondirect routes were reported independently (Refs. 54, 55).
54 K. Susumu, T. Shimidzu, K. Tanaka, and H. Segawa, *Tetrahedron Lett.*, **37**, 8399 (1996).
55 R. G. Khoury, L. Jaquinod, and K. M. Smith, *Chem. Commun.*, **1997**, 1057.
56 J. Wojaczynski, L. Lotos-Grazynski, P. J. Chemielewski, P. V. Calcar, and A. L. Balch, *Inorg. Chem.*, **38**, 3040 (1999).
57 X. Shi and L. S. Liebeskind, *J. Org. Chem.*, **65**, 1665 (2000).
58 M. O. Senge and X. Feng, *Tetrahedron Lett.*, **40**, 4165 (1999).
59 K. Ogawa and Y. Kobuke, *Angew. Chem., Int. Ed.*, **39**, 4070 (2000).
60 A. Osuka, N. Mataga, and T. Okada, *Pure Appl. Chem.*, **69**, 797 (1997).
61 K. Maruyama and A. Osuka, *Pure Appl. Chem.*, **62**, 1511 (1990).
62 K. Maruyama, A. Osuka, and N. Mataga, *Pure Appl. Chem.*, **66**, 867 (1994).
63 A. Osuka, S. Nakajima, K. Maruyama, N. Mataga, T. Asahi, I. Yamazaki, Y. Nishimura, T. Ohno, and K. Nozaki, *J. Am. Chem. Soc.*, **115**, 4577 (1993).
64 A. Osuka, S. Marumo, N. Mataga, S. Taniguchi, T. Okada, I. Yamazaki, Y. Nishimura, T. Ohno, and K. Nozaki, *J. Am. Chem. Soc.*, **118**, 155 (1996).
65 A. Osuka, G. Noya, S. Taniguchi, T. Okada, Y. Nishimura, I. Yamazaki, and N. Mataga, *Chem. Eur. J.*, **6**, 33 (2000).
66 A. Osuka, S. Nakajima, T. Okada, S. Taniguchi, K. Nozaki, T. Ohno, I. Yamazaki, Y. Nishimura, and N. Mataga, *Angew. Chem., Int. Ed. Engl.*, **35**, 92 (1996).
67 S. Kawabata, I. Yamazaki, Y. Nishimura, and A. Osuka, *J. Chem. Soc., Perkin Trans. 2*, **1997**, 479.
68 A. Osuka, M. Ikeda, H. Shiratori, Y. Nishimura, and I. Yamazaki, *J. Chem. Soc., Perkin Trans. 2*, **1999**, 1019.
69 J. E. Baldwin, M. J. Crossley, and J. Debernadis, *Tetrahedron*, **38**, 685 (1982).
70 A. Tsuda, A. Nakano, H. Furuta, H. Yamochi, and A. Osuka, *Angew. Chem., Int. Ed.*, **39**, 558 (2000).
71 K.-i. Sugiura, T. Matsumoto, S. Ohkouchi, Y. Naitoh, T. Kawai, Y. Takai, K. Ushiroda, and Y. Sakata, *Chem. Common.*, **1999**, 1957.
72 A. Tsuda, H. Furuta, and A. Osuka, *Angew. Chem., Int. Ed.*, **39**, 2549 (2000).
73 J. S. Lindsey, I. C. Schreiman, H. C. Hsu, P. C. Kearney, and A. M. Marguerettaz, *J. Org. Chem.*, **52**, 827 (1987).
74 S. G. Dimagno, V. S.-Y. Lin, and M. J. Therien, *J. Org. Chem.*, **58**, 5983 (1993)
75 J.-H. Fuhrhop, E. Baumgartner, and H. Bauer, *J. Am. Chem. Soc.*, **103**, 5854 (1981).
76 A. L. Balch, B. C. Noll, S. M. Reid, and E. P. Zovika, *J. Am. Chem. Soc.*, **115**, 2531 (1993).
77 M. Gouterman, *J. Mol. Spectro.*, **6**, 138 (1961).
78 M. Gouterman, in "The Porphyrins," ed by D. Dolphin, Academic Press, New York (1978), Vol. 3, p. 1.
79 A. Nakano, H. Shimidzu, and A. Osuka, *Tetrahedron Lett.*, **39**, 9489 (1998). Other example, R. W. Boyle, C. K. Johnson, and D. J. Dolphin, *J. Chem. Soc., Chem. Commun.*, **1995**, 527.
80 P. Kovacic and M. B. Jones, *Chem. Rev.*, **87**, 357 (1987).
81 M. Kasha, H. R. Rawls, and M. A. El-Bayoumi, *Pure Appl. Chem.*, **11**, 371 (1965).
82 E. G. McRae and M. Kasha, in "Physical Processes in Radiation Biology," ed by L. Augenstein, R. Mason, and B. Rosenberg, Academic Press, New York (1964), p. 23.
83 M. Kasha, *Radiat. Res.*, **20**, 55 (1963).
84 N. Aratani and A. Osuka, manuscript in preparation.
85 M. Fujita, *Chem. Soc. Rev.*, **27**, 417 (1998).
86 V. Balzani, A. Credi, F. M. Raymo, and J. F. Stoddart, *Angew. Chem., Int. Ed.*, **39**, 3348 (2000).
87 J. M. Lehn, "Supramolecular Chemistry," VCH, Weinheim (1995).
88 V. Thanabal and V. Krishnan, *J. Am. Chem. Soc.*, **104**, 3643 (1982).
89 A. Osuka, N. Tanabe, R. P. Zhang, and K. Maruyama, *Chem. Lett.*, **1993**, 1505.
90 A. Osuka, N. Tanabe, S. Nakajima, and K. Maruyama, *J. Chem. Soc., Perkin Trans. 2*, **1996**, 199.
91 J. L. Sessler, V. L. Capuano, F. M. Raymo, and J. F. Stoddart, *Angew. Chem., Int. Ed. Engl.*, **29**, 1134 (1990).
92 J. L. Sessler, V. L. Capuano, and A. Harriman, *J. Am. Chem. Soc.*, **115**, 4618 (1993).
93 A. Nakano, Thesis, Kyoto University, 2000.
94 A. Nakano, A. Osuka, T. Yamazaki, Y. Nishimura, S. Akimoto, I. Yamazaki, A. Itaya, M. Murakami, and H. Miyasaka, *Chem. Eur. J.*, in press.
95 Oligo-*p*-phenylenevinylene, 11-mer, 8 nm; U. Stalmach, H. Kolshorn, I. Brehm, and H. Meier, *Liebigs Ann.*, **1996**, 1449.
96 Oligo-*p*-phenyleneethynylene, 16-mer, 13 nm; L. Jones II, J. S. Schumm, and J. M. Tour, *J. Org. Chem.*, **62**, 1388 (1997).
97 Oligothiophene, 27-mer, 11 nm; H. Nakanishi, N. Sumi, Y. Aso, and T. Otsubo, *J. Org. Chem.*, **63**, 8632 (1998).
98 Oligothiophenevinylene, 16-mer, 9.5 nm; I. Jestin, P. Frere, P. Blanchard, and J. Roncali, *Angew. Chem., Int. Ed.*, **37**, 942 (1998).
99 Oligothiophene-ethynylene, 17-mer, 13 nm; D. L. Pearson and J. M. Tour, *J. Org. Chem.*, **62**, 1376 (1997).
100 Oligoenediyne, 16-mer, 12 nm; R. E. Martin, T. Mader, and F. Diederich, *Angew. Chem., Int. Ed.*, **38**, 817 (1999).
101 K.-i. Sugiura, H. Tanaka, T. Matsumoto, T. Kawai, and Y. Sakata, *Chem. Lett.*, 1193 (1999).
102 G. Binnig, H. Rohrer, Ch. Gerber, and E. Weibel, *Phys.*

Rev. Lett., **49**, 57 (1982).
103 R. W. Wagner and J. S. Lindsey, *J. Am. Chem. Soc.*, **116**, 9759 (1994).
104 R. W. Wagner, J. S. Lindsey, J. Seth, V. Palaniappan, and D. F. Bocian, *J. Am. Chem. Soc.*, **118**, 3996 (1996).
105 V. Sundström, T. Pullerits, and R. van Grondelle, *J. Phys. Chem. B*, **103**, 2327 (1999).
106 T. Pullerits, M. Chachisvilis, and V. Sundström, *J. Phys. Chem.*, **100**, 10787 (1996).
107 A. M. van Oijen, M. Ketelaars, J. Köhler, T. J. Aartsma, and J. Schmidt, *Science*, **285**, 400 (1999).
108 S. De Boer and D. A. Wiersma, *Chem. Phys. Lett.*, **165**, 45 (1990).
109 P. G. Seybold and M. Gouterman, *J. Mol. Spectro.*, **31**, 1 (1969).
110 M. J. Crossley and P. L. Burn, *J. Chem. Soc., Chem. Commun.*, **1991**, 1569.
111 M. J. Crossley, L. J. Govenlock, and J. K. Praskai, *J. Chem. Soc., Chem. Commun.*, **1995**, 2376.
112 J. R. Reimer, T. X. Lü, M. J. Crossley, and N. S. Hush, *Chem. Phys. Lett.*, **256**, 353 (1996).
113 N. Kobayashi, M. Numao, R. Kondo, S.-I. Nakajima, and T. Osa, *Inorg. Chem.*, **30**, 2241 (1991).
114 L. Jaquinod, C. Gros, M. M. Olmstead, M. Antolovich, and K. M. Smith, *Chem. Commun.*, **1996**, 1475.
115 L. Jaquinod, O. Siri, R. G. Khoury, and K. M. Smith, *Chem. Commun.*, **1998**, 1261.
116 R. Paolesse, L. Jaquinod, F. D. Sala, D. J. Nurco, L. Prodi, M. Montalti, C. D. Natale, A. D'Amico, A. D. Carlo, P. Lugli, and K. M. Smith, *J. Am. Chem. Soc.*, **122**, 11295 (2000).
117 M. G. H. Vicente, M. T. Cancilla, C. B. Lebrilla, and K. M. Smith, *Chem. Commun.*, **1998**, 2355.
118 A. Tsuda and A. Osuka, submitted for publication.

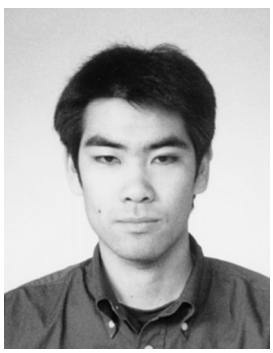

Naoki Aratani was born in 1975 in Nagoya, Japan. He received his B.Sc. and M.Sc. degrees in 1999 and 2001, respectively, from Kyoto University. He is currently a Ph.D. student of Prof. Osuka at the same university, focusing on synthesis of extremely long porphyrin arrays for exploration of the nature of giant molecules. In 2001, he was selected as a Research Fellow of the Japan Society for the Promotion of Science (JSPS).

Atsuhiro Osuka was born in Gamagori, Aichi in 1954. He received his Ph.D. degree from Kyoto University in 1982 on photochemistry of epoxyquinones. In 1979, he started an academic career at the Department of Chemistry of Ehime University as an assistant professor. In 1984, he moved to the Department of Chemistry of Kyoto University, where he became a professor of chemistry in 1996. He was awarded the CSJS Award for Young Chemists in 1988 and the Japanese Photochemistry Association Award in 1999. His research interests cover many aspects of synthetic approaches toward artificial photosynthesis and development of porphyrin-related compounds with novel structures and functions.